

# Core-elements for Least Squares Estimation

Mengyu Li<sup>1</sup>, Jun Yu<sup>\*2</sup>, Tao Li<sup>1</sup>, and Cheng Meng<sup>†1</sup>

<sup>1</sup>Institute of Statistics and Big Data, Renmin University of China, Beijing, China

<sup>2</sup>School of Mathematics and Statistics, Beijing Institute of Technology, Beijing, China

## Abstract

The coresets approach, also called subsampling or subset selection, aims to select a subsample as a surrogate for the observed sample. Such an approach has been used pervasively in large-scale data analysis. Existing coresets methods construct the subsample using a subset of rows from the predictor matrix. Such methods can be significantly inefficient when the predictor matrix is sparse or numerically sparse. To overcome the limitation, we develop a novel element-wise subset selection approach, called core-elements. We provide a deterministic algorithm to construct the core-elements estimator, only requiring an  $O(\text{nnz}(\mathbf{X}) + rp^2)$  computational cost, where  $\mathbf{X} \in \mathbb{R}^{n \times p}$  is the predictor matrix,  $r$  is the number of elements selected from each column of  $\mathbf{X}$ , and  $\text{nnz}(\cdot)$  denotes the number of non-zero elements. Theoretically, we show that the proposed estimator is unbiased and approximately minimizes an upper bound of the estimation variance. We also provide an approximation guarantee by deriving a coresets-like finite sample bound for the proposed estimator. To handle potential outliers in the data, we further combine core-elements with the median-of-means procedure, resulting in an efficient and robust estimator with theoretical consistency guarantees. Numerical studies on various synthetic and real-world datasets demonstrate the proposed method's superior performance compared to mainstream competitors.

*Keywords:* Element-wise subsampling, linear regression, sparse matrix, subset selection.

---

<sup>\*</sup>Joint first author

<sup>†</sup>Corresponding author, chengmeng@ruc.edu.cn

# 1 Introduction

Sparse matrices are matrices in which most of the elements are zero. Such matrices are common in various areas, including medical research, bioinformatics, privacy-preserving analysis, and distributed computing [66; 20; 29; 43]. In these areas, data are usually of high sparsity due to the technical noises, data privacy concerns, and transmission cost, among others [50; 44; 54]. One example is the single-cell RNA-sequencing (scRNA-seq) data containing information about the gene expression level of single cells. Such data are usually expressed in a count matrix, whose rows represent cells and columns represent genes. Owing to technical noises and intrinsic biological variability, scRNA-seq data almost always possess high sparsity, known as the zero-inflation phenomenon [54; 69; 52]. Another example is the word occurrence matrix, whose elements are the so-called TF-IDF values [42]. Here, TF-IDF is short for the term frequency-inverse document frequency, which is calculated by multiplying two metrics, i.e., how many times a word appears in a document, and the inverse document frequency of the word across a set of documents. As a result, TF-IDF is a highly sparse matrix for a short document and a large language model that contains millions of words [68; 67].

In reality, many sparse matrices also exist due to missing values, i.e., the elements are not fully observed. Numerous methods have been developed to deal with the missing values in such cases, and most of these methods aim to fill the sparse matrix with some estimated non-zero values [13; 75; 71; 37; 65]. In this paper, however, we are less concerned with missing values and instead focus on the case that the sparse matrix itself is fully observed.

We consider large-scale data analysis where the predictor matrix is highly sparse. One widely-used technique for large-scale data analysis is the coresets method, also called sub-sampling or subset selection. These methods select a subsample as a surrogate for the observed sample. Recently, such methods have been used pervasively in data reduction, measurement-constrained analysis, and active learning [70; 57; 61; 51]. Various coresets

methods have been proposed for linear regression [19; 12; 57; 60; 86; 58; 21; 18], generalized linear regression [77; 3; 85; 4], streaming time series [83; 49], large-scale matrix approximation [82; 80; 5; 7; 79], nonparametric regression [33; 55; 86; 63; 72; 62], among others.

Despite the wide application, most existing coresets methods mainly focus on dense predictor matrices, and may be inefficient when the predictor matrix is of high sparsity. In particular, most of these methods construct the subsample using certain rows from the observed sample. When the observed predictor matrix is sparse, the selected subsample matrix also tends to be sparse. Such a subsample thus may lead to inefficient results, since the selected zero-valued elements have almost no impact on the down-streaming analysis, such as model estimation, prediction, and inference. More efficient statistical tools that are suitable for sparse matrices are still meager.

In this paper, we bridge the gap by developing a novel element-wise subset selection method, called core-elements, for large-scale least squares estimation. Different from the existing coresets methods that aim to select  $r$  rows from the predictor matrix  $\mathbf{X} \in \mathbb{R}^{n \times p}$  ( $n \gg p$ ), we aim to construct a sparser sketch  $\mathbf{X}^*$  by keeping  $rp$  elements of  $\mathbf{X}$  and zeroing out the remaining elements. Loosely speaking, our approach generalizes the existing coresets methods by getting rid of the requirement that the selected  $rp$  elements have to be located in  $r$  rows. We provide a deterministic algorithm to construct the core-elements estimator. Utilizing such an estimator, we can approximate the least squares estimation within  $O(\text{nnz}(\mathbf{X}) + rp^2)$  computational time, where  $\text{nnz}(\cdot)$  denotes the number of non-zero elements. Theoretically, we show that the proposed estimator is unbiased to the true coefficient, and it approximately minimizes an upper bound of the estimation variance.

We also provide a coresets-like finite sample bound for the proposed estimator with approximation guarantees. Let  $\mathbf{y} \in \mathbb{R}^n$  be the response,  $\hat{\boldsymbol{\beta}}_{\text{OLS}}$  be the full sample least squares estimator, and  $\tilde{\boldsymbol{\beta}}$  be the proposed estimator. Let  $\|\cdot\|$  be the Euclidean norm of a vector and  $\|\cdot\|_2$  be the spectral norm of a matrix. We show that to achieve the

$(1 + \epsilon)$ -relative error, i.e.,

$$\|\mathbf{y} - \mathbf{X}\hat{\boldsymbol{\beta}}_{\text{OLS}}\|^2 \leq \|\mathbf{y} - \mathbf{X}\tilde{\boldsymbol{\beta}}\|^2 \leq (1 + \epsilon)\|\mathbf{y} - \mathbf{X}\hat{\boldsymbol{\beta}}_{\text{OLS}}\|^2,$$

the proposed estimator requires a sketch  $\mathbf{X}^*$  such that the ratio  $\|\mathbf{X} - \mathbf{X}^*\|_2 / \|\mathbf{X}\|_2$  is  $O(\epsilon^{1/2})$ . Intuitively, such a result indicates that when the predictor matrix  $\mathbf{X}$  gets (numerically) sparser, fewer elements are required in the sketch  $\mathbf{X}^*$  to achieve the  $(1 + \epsilon)$ -relative error.

To handle potential outliers in the data, we develop a robust variant of the core-element method by integrating it with the popular median-of-means procedure [41; 6; 53; 47; 74]. We further propose an algorithm to construct the robust estimator within  $O(\text{nnz}(\mathbf{X}) + rp^2)$  time. Theoretically, we show that the robust estimator is consistent with the true coefficient under certain regularity conditions.

To evaluate the empirical performance and computational time of the proposed strategy, we compare it with several mainstream competitors through extensive synthetic and real-world datasets, including uncorrupted and corrupted datasets with dense or sparse predictor matrices. Interestingly, although the proposed estimator is mainly designed for sparse matrices, numerical results show it significantly outperforms the competitors respecting both estimation error and CPU time even when the predictor matrix is dense.

The remainder of this paper is organized as follows. We start in Section 2 by introducing the linear model and the state-of-the-art subsampling methods. In Section 3, we develop a core-elements estimator and present its theoretical properties. The robust version of the core-elements estimator is introduced in Section 4. We examine the performance of the proposed estimators through extensive simulations and two real data examples in Sections 5 and 6, respectively. The technical proofs are provided in the Supplementary Material.

## 2 Background

In the following, we adopt the common convention of using uppercase boldface letters for matrices, lowercase boldface letters for vectors, and regular font for scalars. For a vector  $\mathbf{x} = (x_1, \dots, x_n) \in \mathbb{R}^n$ , define its Euclidean norm by  $\|\mathbf{x}\|$ . For a matrix  $\mathbf{X} = (x_{ij}) \in \mathbb{R}^{n_1 \times n_2}$ , its spectral norm (i.e., the largest singular value) and Frobenius norm are denoted as  $\|\mathbf{X}\|_2$  and  $\|\mathbf{X}\|_F$ , respectively.

### 2.1 Subsampling methods for least squares estimation

Consider the linear model,

$$y_i = \mathbf{x}_i^\top \boldsymbol{\beta} + \varepsilon_i, \quad i = 1, \dots, n. \quad (1)$$

Here  $\{y_i\}_{i=1}^n \in \mathbb{R}$  are the responses,  $\{\mathbf{x}_i\}_{i=1}^n \in \mathbb{R}^p$  are the observations,  $\boldsymbol{\beta} \in \mathbb{R}^p$  is a vector of unknown coefficients, and  $\{\varepsilon_i\}_{i=1}^n$  are i.i.d. error terms with zero mean and constant variance  $\sigma^2$ . Let  $\mathbf{y} = (y_1, \dots, y_n) \in \mathbb{R}^n$  be the response vector,  $\mathbf{X} = (\mathbf{x}_1, \dots, \mathbf{x}_n)^\top \in \mathbb{R}^{n \times p}$  be the predictor matrix, and  $\boldsymbol{\varepsilon} = (\varepsilon_1, \dots, \varepsilon_n) \in \mathbb{R}^n$  be the noise vector. In this study, we assume that  $n \gg p$ ,  $p$  is fixed, and  $\mathbf{X}$  is of full column rank. It is widely-known that the ordinary least squares (OLS) estimator of  $\boldsymbol{\beta}$  takes the form

$$\hat{\boldsymbol{\beta}}_{\text{OLS}} = (\mathbf{X}^\top \mathbf{X})^{-1} \mathbf{X}^\top \mathbf{y}. \quad (2)$$

In practice, the calculation of the least squares problem may suffer from high computational costs. Specifically, standard computation of the formulation (2) requires  $O(np^2)$  computational time, which can be considerable when both  $n$  and  $p$  are large. To tackle the computational burden, various subsampling methods have been proposed. The main idea of subsampling methods can be described as follows: given a predictor matrix  $\mathbf{X} \in \mathbb{R}^{n \times p}$ , subsample  $r$  rows (i.e.,  $r$  observations) from  $\mathbf{X}$  to construct a much smaller sketch  $\hat{\mathbf{X}} \in \mathbb{R}^{r \times p}$ , and then use it as a surrogate for  $\mathbf{X}$  in down-streaming analysis.

Most of the existing subsampling methods can be divided into two classes, i.e., the randomized subsampling approach and the design-based subsampling approach. The former class aims to carefully design a data-dependent non-uniform sampling probability distribution such that more informative data points will be selected with larger sampling weights [56; 60; 86; 58]. In contrast, the latter class aims to construct the most effective subsample estimator based on certain optimality criteria developed in the design of experiments [81; 76; 61; 78]. We refer to [51] for a recent review.

Close related to the subsampling methods are the coresets methods. These methods aim to select a subsample in a deterministic way, such that a loss function  $\mathcal{L}$  based on the subsample estimator is bounded by the loss function based on the full-sample estimator multiplying a constant  $(1 + \epsilon)$  [30; 12; 64; 31]. In least squares estimation, a subsample  $\widehat{\mathbf{X}}$  is called an  $(1 + \epsilon)$ -coreset ( $\epsilon > 0$ ), if there exists an estimator  $\widetilde{\boldsymbol{\beta}}$  constructed by  $\widehat{\mathbf{X}}$ , such that

$$\|\mathbf{y} - \mathbf{X}\widehat{\boldsymbol{\beta}}_{\text{OLS}}\|^2 \leq \|\mathbf{y} - \mathbf{X}\widetilde{\boldsymbol{\beta}}\|^2 \leq (1 + \epsilon)\|\mathbf{y} - \mathbf{X}\widehat{\boldsymbol{\beta}}_{\text{OLS}}\|^2.$$

## 2.2 Sparse and numerically sparse matrices

Recall that sparse matrices are matrices in which most elements are zero. Commonly, the sparsity is measured by using the  $\ell_0$  norm. Such a procedure, however, may not accurately reflect the simplicity of nearly sparse instances with a large number of small but non-zero elements. To combat the obstacle, existing literature also considers the so-called numerically sparse matrices [34]. Intuitively, numerically sparse is a weaker condition than sparse in which we do not require most elements to be zero, only that most elements are small enough to be ignored. Examples of numerically sparse are widely encountered in practice, including but not limited to linear programming constraints of the form  $x_1 \geq \sum_{i=1}^n x_i/n$ , and physical models whose strength of interaction decays with distance [16].

## 2.3 Element-wise sampling on sparse data matrices

Consider the scenario that the observed predictor matrix  $\mathbf{X} \in \mathbb{R}^{n \times p}$  is a (numerically) sparse matrix in which most of the elements are (nearly) zero. Oftentimes, of interest is to find a sparser sketch  $\mathbf{X}^+ \in \mathbb{R}^{n \times p}$  that is a good proxy for  $\mathbf{X}$ . Here,  $\mathbf{X}^+$  is also a sparse matrix, from which the non-zero elements are a subset of the non-zero elements with respect to (w.r.t.)  $\mathbf{X}$ . The problem of finding such a matrix  $\mathbf{X}^+$  has many applications in eigenvector approximation [9; 2; 28; 45; 34], semi-definite programming [8; 26; 32], and matrix completion [14; 15; 17].

To construct such a matrix  $\mathbf{X}^+$ , most existing methods aim to design a good sampling probability distribution, such that the approximation error  $\|\mathbf{X} - \mathbf{X}^+\|_2$  is as small as possible. Let  $s$  be the number of selected non-zero elements, and  $p_{ij}$  ( $i = 1, \dots, n, j = 1, \dots, p$ ) be the sampling probability. [2] proposed the so-called  $\ell_2$  sampling such that  $p_{ij} \propto x_{ij}^2$ , and provided theoretical bounds for this approach. These bounds were later refined by [25]. Alternatively, [9] proposed  $\ell_1$  sampling, where  $p_{ij} \propto |x_{ij}|$ . Later, [1] proposed a near-optimal probability distribution using matrix-Bernstein inequality. Their approach can be regarded as a combination of two  $\ell_1$ -based distributions. In particular,  $p_{ij} \propto |x_{ij}|$  when  $s$  is small, and  $p_{ij} \propto |x_{ij}| \cdot \|\mathbf{x}_i\|_1$  as  $s$  grows, where  $\|\cdot\|_1$  denotes the  $\ell_1$  norm of a vector. More recently, [45] developed hybrid- $(\ell_1, \ell_2)$  sampling, which is also a convex combination of probabilities.

In general, existing literature on element-wise sampling mainly focus on the algorithmic perspective, such that the applications of interest are usually compressed sensing and matrix recovery. Nevertheless, element-wise sampling with a statistical perspective, such that the applications involve providing effective and efficient solutions for large-scale statistical modeling and inference, is still a blank field and remains further studied.

### 3 Core-elements

In this section, we present our main algorithm and the theoretical properties of the proposed estimator. We first introduce the definition of the core-elements and then develop an unbiased core-elements estimator. Next, we provide an upper bound for the variance of such an estimator by utilizing the matrix-form Taylor expansion. We then provide an algorithm for core-elements selection, resulting in an estimator that approximately minimizes this upper bound. A coresets-like finite sample bound is then provided to quantify the approximation error for the proposed estimator. The technical proofs are relegated to Supplementary Material.

#### 3.1 Problem setup

We consider the problem of large-scale least squares estimation when the predictor matrix  $\mathbf{X}$  is sparse or numerically sparse. To utilize the sparse structure, we propose to construct a sparser sketch  $\mathbf{X}^* \in \mathbb{R}^{n \times p}$  from  $\mathbf{X}$  carefully, and use  $\mathbf{X}^*$  to construct an efficient least squares approximation. In particular, given a positive integer  $s$ , let  $\mathbf{S}$  be an  $n \times p$  matrix such that its elements involves  $s$  ones and  $np - s$  zeros. The sketch  $\mathbf{X}^*$  then can be formulated as  $\mathbf{X}^* = \mathbf{S} \odot \mathbf{X}$ , where  $\odot$  represents the Hadamard product, i.e., element-wise product. In other words,  $\mathbf{X}^*$  is produced by keeping  $s$  elements of  $\mathbf{X}$  and zeroing out the remaining elements. We then propose a general estimator that takes the form

$$\tilde{\boldsymbol{\beta}}(\mathbf{D}) = \mathbf{D}\mathbf{X}^{*\top}\mathbf{y}, \quad (3)$$

where  $\mathbf{D} \in \mathbb{R}^{p \times p}$  is a scaling matrix to be determined.

A natural question arises: given a fixed budget  $s$ , among all the estimators that take the form (3), how to construct the scaling matrix  $\mathbf{D}$  and the sparse sketch  $\mathbf{X}^*$ , such that (I) the estimator  $\tilde{\boldsymbol{\beta}}(\mathbf{D})$  is unbiased and (II) its estimation variance is as small as possible? For the first part of this question, one can see that when  $\mathbf{D} = (\mathbf{X}^{*\top}\mathbf{X})^{-1}$ ,  $\mathbb{E}(\tilde{\boldsymbol{\beta}}(\mathbf{D})) =$



$(\mathbf{X}^{*\top} \mathbf{X})^{-1} \mathbf{X}^{*\top} (\mathbf{X} \boldsymbol{\beta} + \mathbb{E}(\boldsymbol{\varepsilon})) = \boldsymbol{\beta}$ , indicating that  $\tilde{\boldsymbol{\beta}}(\mathbf{D})$  is unbiased to  $\boldsymbol{\beta}$ . Such a finding motivates us to focus on the unbiased estimator

$$\tilde{\boldsymbol{\beta}} = (\mathbf{X}^{*\top} \mathbf{X})^{-1} \mathbf{X}^{*\top} \mathbf{y}.$$

Consider the classical subsample-based estimator

$$\tilde{\boldsymbol{\beta}}' = (\hat{\mathbf{X}}^\top \hat{\mathbf{X}})^{-1} \hat{\mathbf{X}}^\top \mathbf{y},$$

where  $\hat{\mathbf{X}} \in \mathbb{R}^{r \times p}$  represents a subsample. When the selected  $s = rp$  elements locate in  $r$  rows, i.e., when the element-wise subset selection degenerates to the row selection, it can be shown that  $\tilde{\boldsymbol{\beta}} = \tilde{\boldsymbol{\beta}}'$ . While in general cases, these two estimators are different.

Next, we consider the variance of the estimator  $\tilde{\boldsymbol{\beta}}$ . Recall that  $\sigma^2$  represents the variance of random errors in model (1). Our goal is to find a sketch  $\mathbf{X}^*$  that minimizes the estimation variance, which has a closed form

$$\begin{aligned} \mathbb{E}(\|\tilde{\boldsymbol{\beta}} - \boldsymbol{\beta}\|^2) &= \mathbb{E}(\mathbf{y}^\top \mathbf{X}^* (\mathbf{X}^\top \mathbf{X}^*)^{-1} (\mathbf{X}^{*\top} \mathbf{X})^{-1} \mathbf{X}^{*\top} \mathbf{y}) - \boldsymbol{\beta}^\top \boldsymbol{\beta} \\ &= \boldsymbol{\beta}^\top \boldsymbol{\beta} + \sigma^2 \text{tr}(\mathbf{X}^* (\mathbf{X}^\top \mathbf{X}^*)^{-1} (\mathbf{X}^{*\top} \mathbf{X})^{-1} \mathbf{X}^{*\top}) - \boldsymbol{\beta}^\top \boldsymbol{\beta} \\ &= \sigma^2 \|(\mathbf{X}^{*\top} \mathbf{X})^{-1} \mathbf{X}^{*\top}\|_F^2. \end{aligned} \tag{4}$$

However, this variance term is challenging to minimize directly. To combat the obstacle, we provide an upper bound for (4) and aim to minimize the upper bound instead. The upper bound is derived by utilizing the matrix-form Taylor expansion (see Chapter 1, [38]), detailed in Lemma 1.

**Lemma 1.** *Let  $\mathbf{L} = \mathbf{X} - \mathbf{X}^*$ . A Taylor expansion of  $\mathbb{E}(\|\tilde{\boldsymbol{\beta}} - \boldsymbol{\beta}\|^2)$  around the point  $\mathbf{X}^* = \mathbf{X}$  yields the following upper bound,*

$$\mathbb{E}(\|\tilde{\boldsymbol{\beta}} - \boldsymbol{\beta}\|^2) \leq \sigma^2 p \left[ \text{tr}((\mathbf{X}^\top \mathbf{X})^{-1}) \left\{ (p + \text{tr}((\mathbf{X}^\top \mathbf{X})^{-1}) \|\mathbf{L}\|_F^2) (1 + O(\lambda_0)) \right\} \right]. \tag{5}$$

Here, assume that the spectral radius  $\lambda_0 = \|(\mathbf{X}^\top \mathbf{X})^{-1} \mathbf{L}^\top \mathbf{X}\|_2 < 1$  to ensure the convergence of the matrix series.

When the Taylor expansion in Lemma 1 is valid, the inequality (5) indicates that the upper bound of the estimation variance decreases as  $\|\mathbf{L}\|_F$  and the remainder  $\lambda_0$  decreases. Considering  $\lambda_0$ , we have

$$\begin{aligned}\lambda_0 &\leq \|(\mathbf{X}^\top \mathbf{X})^{-1}\|_2 \|\mathbf{X}\|_2 \|\mathbf{L}\|_2 \\ &\leq \|(\mathbf{X}^\top \mathbf{X})^{-1}\|_2 \|\mathbf{X}\|_2 \left( p \max_{j \in \{1, \dots, p\}} \mathbf{L}^{(j)\top} \mathbf{L}^{(j)} \right)^{1/2},\end{aligned}$$

where  $\mathbf{L}^{(j)}$  denotes the  $j$ th column of  $\mathbf{L}$ . Such an inequality indicates that a smaller value of the maximum column norm of  $\mathbf{L}$  is associated with a smaller  $\lambda_0$ . As a result, to minimize the upper bound in Lemma 1, we need to keep both  $\|\mathbf{L}\|_F$  and the column norms of  $\mathbf{L}$  as small as possible.

Motivated by this, we propose to construct  $\mathbf{X}^*$  by keeping the elements with the top largest absolute values w.r.t. each column of  $\mathbf{X}$  and zeroing out the remainings. Intuitively, for a fixed number of selected elements, such  $\mathbf{L}$  has the approximately minimum column norm respecting every column. Thus, both the values of  $\|\mathbf{L}\|_F$  and  $\|\mathbf{L}\|_2$  will be approximately minimized, resulting in a relatively small upper bound of the estimation variance in Lemma 1. We call such a procedure “core-elements” since the idea behind it is analogous to “coresets”, except that what we select are elements instead of rows.

## 3.2 Main algorithm

Without loss of generality, we assume the number of selected elements  $s = rp$ , where  $r$  is an integer. Algorithm 1 summarizes the construction of core-elements and the proposed estimator, which are illustrated in Fig. 1.

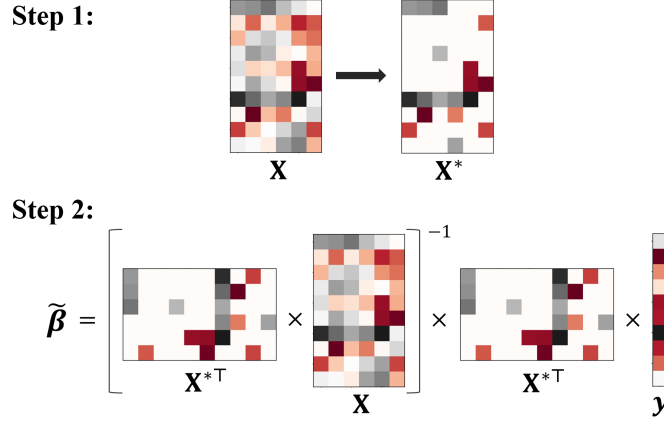


Figure 1: Illustration for Algorithm 1. Each element of a matrix is labeled by a different color, such that larger positive and smaller negative values are labeled by more red and more black colors, respectively. **Step 1** illustrates the core-elements selection, where  $r = 3$  elements with the largest absolute values w.r.t. each column are selected. **Step 2** illustrates the proposed estimator.

---

**Algorithm 1** CORE-ELEMENTS( $\mathbf{X}, \mathbf{y}, r$ )

---

- 1: **Input:**  $\mathbf{X} = (x_{ij}) \in \mathbb{R}^{n \times p}$ ,  $\mathbf{y} \in \mathbb{R}^n$ ,  $r \in \mathbb{Z}_+$
  - 2: Initialize  $\mathbf{S} = (\mathbf{0}) \in \mathbb{R}^{n \times p}$
  - 3: **for**  $j = 1, \dots, p$  **do**
  - 4:   Let  $\mathcal{I} = \{i_1, \dots, i_r\}$  be an index set, such that  $\{|x_{i_q j}|\}_{q=1}^r$  are the  $r$  largest ones among  $\{|x_{ij}|\}_{i=1}^n$
  - 5:   Let  $s_{i_q j} = 1$ ,  $q = 1, \dots, r$
  - 6: **end for**
  - 7:  $\mathbf{X}^* = \mathbf{S} \odot \mathbf{X}$ , where  $\odot$  represents the element-wise product
  - 8: **Return**  $\tilde{\boldsymbol{\beta}} = (\mathbf{X}^{*\top} \mathbf{X})^{-1} \mathbf{X}^{*\top} \mathbf{y}$
- 

Consider the computational cost of Algorithm 1. Constructing the matrix  $\mathbf{X}^*$  requires  $O(\text{nnz}(\mathbf{X}))$  time. Note that each column of  $\mathbf{X}^*$  contains at most  $r$  non-zero elements, thus calculating  $\mathbf{X}^{*\top} \mathbf{X}$  takes  $O(rp^2)$  time. The computing time for  $\tilde{\boldsymbol{\beta}}$  is thus at the order of  $O(rp^2 + p^3)$ . Therefore, the overall computational cost of Algorithm 1 is  $O(\text{nnz}(\mathbf{X}) + rp^2)$ , which becomes  $O(\text{nnz}(\mathbf{X}))$  when  $n \gg r$ . In the large-sample scenario such that  $n \gg p$ , such an algorithm is much faster than the popular leverage-based subsampling methods [56]. This is because the leverage-based methods involve the singular value decomposition

of the full predictor matrix, requiring a cost of the order  $O(np^2)$ .

### 3.3 Theoretical properties

We now present our main theorem, indicating that the selected elements are  $(1 + \epsilon)$ -core-elements for least squares estimation. In other words, under some regularity conditions, the proposed estimate achieves a  $(1 + \epsilon)$ -relative error w.r.t. the  $\ell_2$  loss.

**Theorem 2.** *Given  $\mathbf{X} \in \mathbb{R}^{n \times p}$ ,  $\mathbf{y} \in \mathbb{R}^n$  and  $\epsilon > 0$ , let  $\mathbf{X}^*$  be the sketch matrix and  $\tilde{\boldsymbol{\beta}}$  be the estimate that calculated by Algorithm 1. Let  $\kappa(\mathbf{X}) = \sigma_{\max}(\mathbf{X})/\sigma_{\min}(\mathbf{X})$  be the condition number, where  $\sigma_{\max}(\cdot)$  and  $\sigma_{\min}(\cdot)$  respectively stand for the maximum and minimum singular values. When  $\mathbf{X}^*$  satisfies  $\|\mathbf{X} - \mathbf{X}^*\|_2 \leq \epsilon' \|\mathbf{X}\|_2$  with*

$$0 < \epsilon' \leq \frac{1}{\kappa^2(\mathbf{X})} \left( 1 + \frac{(\kappa^2(\mathbf{X}) + 1) \|\mathbf{y}\|}{\epsilon^{1/2} \|\mathbf{y} - \mathbf{X} \hat{\boldsymbol{\beta}}_{\text{OLS}}\|} \right)^{-1}, \quad (6)$$

*we have*

$$\|\mathbf{y} - \mathbf{X} \hat{\boldsymbol{\beta}}_{\text{OLS}}\|^2 \leq \|\mathbf{y} - \mathbf{X} \tilde{\boldsymbol{\beta}}\|^2 \leq (1 + \epsilon) \|\mathbf{y} - \mathbf{X} \hat{\boldsymbol{\beta}}_{\text{OLS}}\|^2. \quad (7)$$

Theorem 2 indicates that to achieve the  $(1 + \epsilon)$ -relative error in inequality (7), Algorithm 1 requires a sketch  $\mathbf{X}^*$  such that the ratio  $\|\mathbf{X} - \mathbf{X}^*\|_2 / \|\mathbf{X}\|_2$  is  $O(\epsilon^{1/2})$ . This rate is supported by empirical results in Section 5. Intuitively, such a result also indicates that when the predictor matrix  $\mathbf{X}$  gets (numerically) sparser, fewer elements are required in the sketch  $\mathbf{X}^*$  to achieve the same relative error w.r.t. the  $\ell_2$  loss.

In addition, the value of  $\epsilon'$  also depends on the condition number  $\kappa(\mathbf{X})$ , and the relative sum of squares error (SSE)  $\|\mathbf{y} - \mathbf{X} \hat{\boldsymbol{\beta}}_{\text{OLS}}\|^2 / \|\mathbf{y}\|^2$ . Specifically, a larger  $\epsilon'$  is admitted to achieve the  $(1 + \epsilon)$ -relative error if the condition number  $\kappa(\mathbf{X})$  decreases and the SSE increases.

## 4 MOM Core-elements

To guarantee the robustness of the core-elements approach, we modify Algorithm 1 by combining it with the popular median-of-means (MOM) procedure [41; 6; 39; 53; 46; 48; 47; 74; 59] to provide a robust version of core-elements, called “MOM core-elements”. We first propose an algorithm in the divide-and-conquer framework to obtain the MOM core-elements estimator, and then we establish consistency of the proposed estimator under regularity conditions.

### 4.1 Proposed algorithm

Due to the existence of outliers, we relax the standard i.i.d. setup to the  $\mathcal{I} \cup \mathcal{O}$  framework following [47]. Specifically, we assume that data are partitioned into two (unknown) sets,  $\mathcal{I}$  and  $\mathcal{O}$ , such that  $\mathcal{I} \cup \mathcal{O} = \{1, \dots, n\}$  and  $\mathcal{I} \cap \mathcal{O} = \emptyset$ . Data  $\{(\mathbf{x}_i, y_i)\}_{i \in \mathcal{I}}$  are i.i.d. informative data, and data  $\{(\mathbf{x}_i, y_i)\}_{i \in \mathcal{O}}$  are outliers on which no assumption is granted.

Given a random partition of the full data  $(\mathbf{X}, \mathbf{y}) = \{(\mathbf{x}_i, y_i)\}_{i=1}^n$  into blocks of equal sizes, the principle of MOM estimator is that we first obtain an estimation on each block independently, and then we aggregate the results from these blocks by taking the median. Let  $k$  be the number of blocks and  $n_k = \lfloor n/k \rfloor$  be the size of each block. Denote  $(\mathbf{X}^{(l)}, \mathbf{y}^{(l)}) \in \mathbb{R}^{n_k \times p} \times \mathbb{R}^{n_k}$  be the data partitioned into the  $l$ th block. For the  $l$ th block, we construct the core-elements matrix  $\mathbf{X}^{(l)*}$  containing  $\lfloor s/k \rfloor$  non-zero elements and obtain the corresponding estimator  $\tilde{\boldsymbol{\beta}}^{(l)} = (\mathbf{X}^{(l)*\top} \mathbf{X}^{(l)})^{-1} \mathbf{X}^{(l)*\top} \mathbf{y}^{(l)}$ . Then, the MOM core-elements estimator is defined as

$$\tilde{\boldsymbol{\beta}}_{\text{MOM}} = \text{med}(\tilde{\boldsymbol{\beta}}^{(1)}, \dots, \tilde{\boldsymbol{\beta}}^{(k)}), \quad (8)$$

where  $\text{med}(\cdot)$  denotes the coordinate-wise median. Algorithm 2 details the MOM core-elements procedure.

---

**Algorithm 2** MOM CORE-ELEMENTS( $\mathbf{X}, \mathbf{y}, r, k$ )

---

```
1: Input:  $\mathbf{X} = (x_{ij}) \in \mathbb{R}^{n \times p}$ ,  $\mathbf{y} \in \mathbb{R}^n$ ,  $r, k \in \mathbb{Z}_+$ 
2: Partition  $(\mathbf{X}, \mathbf{y})$  into  $k$  blocks  $\{(\mathbf{X}^{(l)}, \mathbf{y}^{(l)})\}_{l=1}^k$  randomly and evenly
3: for  $l = 1, \dots, k$  do
4:   Compute  $\tilde{\boldsymbol{\beta}}^{(l)} = \text{CORE-ELEMENTS}(\mathbf{X}^{(l)}, \mathbf{y}^{(l)}, \lfloor r/k \rfloor)$ 
5: end for
6: Return  $\tilde{\boldsymbol{\beta}}_{\text{MOM}} = \text{med}(\tilde{\boldsymbol{\beta}}^{(1)}, \dots, \tilde{\boldsymbol{\beta}}^{(k)})$ 
```

---

In Algorithm 2, the number of blocks  $k$  indicates the robustness of our proposed estimator. A popular measure to quantify robustness is the breakdown point [36; 23; 22; 47], defined as the smallest proportion of corrupted observations needed to push an estimator to infinity. The breakdown point of Algorithm 2 is  $\lfloor k/2 \rfloor / n$ , because less than  $\lfloor k/2 \rfloor$  outliers may corrupt at most  $\lfloor k/2 \rfloor$  blocks, leaving the median in (8) equals to the estimation on a single block with uncorrupted data. Remark that Algorithm 1 is a special case of Algorithm 2 where  $k = 1$ , which is applicable to datasets without extreme outliers.

Consider the computation time of Algorithm 2. Constructing the core-elements estimator on a single block requires  $O(\text{nnz}(\mathbf{X})/k + rp^2/k + p^3)$  time, and the aggregation step needs  $O(kp)$  time. Thus, the total computational cost of Algorithm 2 is at the order of  $O(\text{nnz}(\mathbf{X}) + rp^2 + kp^3 + kp) = O(\text{nnz}(\mathbf{X}) + rp^2)$ , where the equation holds because  $r/k$  should be at least of the same order as  $p$  for ensuring the well-definedness of  $\tilde{\boldsymbol{\beta}}^{(1)}, \dots, \tilde{\boldsymbol{\beta}}^{(k)}$ . Such cost is the same as that of Algorithm 1.

## 4.2 Theoretical properties

Now we provide the convergence of the MOM core-elements estimator. To begin with, we introduce the following regularity conditions.

(H.1) Denote the Fisher information matrix  $\mathbf{I}^{(l)} = n_k^{-1} \mathbf{X}^{(l)\top} \mathbf{X}^{(l)}$  on the  $l$ th block. Assume that  $c < \inf_l \lambda_{\min}(\mathbf{I}^{(l)}) \leq \sup_l \lambda_{\max}(\mathbf{I}^{(l)}) < \infty$  for some constant  $c > 0$ , where  $\lambda_{\max}(\cdot)$  and  $\lambda_{\min}(\cdot)$  respectively stand for the maximum and minimum eigenvalues.

(H.2) Let  $\mathbf{L}^{(l)} = \mathbf{X}^{(l)} - \mathbf{X}^{(l)*}$ . Assume that  $\sup_l \|\mathbf{L}^{(l)}\|_F^2 / n_k^2 \rightarrow 0$ .

(H.3) Assume that the spectral radius  $\lambda_0^{(l)} = \|(\mathbf{X}^{(l)\top} \mathbf{X}^{(l)})^{-1} \mathbf{L}^{(l)\top} \mathbf{X}^{(l)}\|_2 < 1$  for any  $l \in \{1, \dots, k\}$ .

(H.4) Suppose that  $k > 2|\mathcal{B}_\mathcal{O}| + 1$ , where  $\mathcal{B}_\mathcal{O}$  is the set of blocks containing at least one outlier and  $|\cdot|$  denotes the cardinal number. Further assume that  $\mathcal{B}_\mathcal{O}$  contains finite elements.

**Theorem 3.** *Under the conditions (H.1)–(H.4), as  $k, n_k \rightarrow \infty$ ,  $\tilde{\boldsymbol{\beta}}_{\text{MOM}}$  converges to  $\boldsymbol{\beta}$  in probability, i.e., for any given  $\epsilon > 0$ , it holds that*

$$\mathbb{P}(\|\tilde{\boldsymbol{\beta}}_{\text{MOM}} - \boldsymbol{\beta}\| > \epsilon) \rightarrow 0.$$

In Theorem 3, condition (H.1) is commonly assumed in the literature. Conditions (H.2) and (H.3) bound the error of the local core-elements estimator on each block by using Lemma 1. Condition (H.4) guarantees the effectiveness of the MOM procedure according to its breakdown point discussed above.

## 5 Simulation Study

In this section, we first evaluate the performance of core-elements (i.e., Algorithm 1) in estimating  $\boldsymbol{\beta}$  and predicting  $\mathbf{y}$  on uncorrupted synthetic datasets. We then provide empirical evidence to support the error bound in Theorem 2. Next, we consider corrupted datasets to show the effectiveness and robustness of MOM core-elements (i.e., Algorithm 2). Finally, we show the advantage of the proposed strategy over other subsampling methods w.r.t. the computational time.

## 5.1 Performance on uncorrupted data

We use CORE to refer to the estimator in Algorithm 1. For comparison, we consider several state-of-the-art subsampling methods including uniform subsampling (UNIF), basic leverage subsampling (BLEV) [24; 56], shrinkage leverage subsampling (SLEV) with parameter  $\alpha = 0.9$  [56], and information-based optimal subset selection (IBOSS) [76].

For uncorrupted data, the predictor matrix  $\mathbf{X}$  is generated from different kinds of widely-used distributions:

**D1.** multivariate normal distribution,  $N(\mathbf{0}, \Sigma)$ ;

**D2.** multivariate log-normal distribution,  $LN(\mathbf{0}, \Sigma)$ ;

**D3.** multivariate t-distribution with 3 degrees of freedom,  $t_3(\mathbf{0}, \Sigma)$ ,

where  $\Sigma = (\sigma_{ij}) \in \mathbb{R}^{p \times p}$  is a covariance matrix with  $\sigma_{ij} = 0.6^{|i-j|}$  for  $i, j \in \{1, \dots, p\}$ .

In order to introduce sparsity, after generating the predictor matrices, we first randomly zero out their elements with a sparsity ratio  $\alpha$ . Specifically, we randomly select  $\alpha \times 100\%$  of the elements and set these elements to be zero. Consider  $\alpha = \{0, 0.2, 0.4, 0.6, 0.8\}$ , referred to as **R1-R5**, respectively. Next, we add a small random perturbation to each zero element of the predictor matrix to obtain a numerically sparse matrix. Note that **R1** corresponds to a completely dense matrix, and **R5** corresponds to a highly numerically sparse matrix. We then generate the response  $\mathbf{y}$  from the linear model (1). The true coefficient  $\beta$  is a  $p$ -dimensional vector of unity, and the signal-to-noise ratio, defined as  $\text{SNR} = \text{Var}(\mathbf{X}\beta)/\sigma^2$ , is set to be 4. Let the sample size  $n = 10^4$  and dimension  $p = 100$ . For the row-sampling methods, i.e., UNIF, BLEV, SLEV, and IBOSS, we select  $r \in \{2p, 4p, \dots, 10p\}$  rows for each of these methods. For a fair comparison, we select  $s = rp$  elements for the proposed core-elements method.

We calculate the empirical mean squared error (MSE) for each of the estimator based



on 100 replications, i.e.,

$$\text{MSE} = \frac{1}{100} \sum_{i=1}^{100} \frac{\|\widehat{\boldsymbol{\beta}}^{(i)} - \boldsymbol{\beta}\|^2}{\|\boldsymbol{\beta}\|^2}, \quad (9)$$

where  $\widehat{\boldsymbol{\beta}}^{(i)}$  represents the estimator in the  $i$ th replication. We also consider the prediction MSE (PMSE). For the  $i$ th replication, we randomly split the observed sample into a training set  $(\mathbf{y}_{\text{train}}^{(i)}, \mathbf{X}_{\text{train}}^{(i)})$  of size  $\lfloor 0.7n \rfloor$  and a test set  $(\mathbf{y}_{\text{test}}^{(i)}, \mathbf{X}_{\text{test}}^{(i)})$  of size  $\lfloor 0.3n \rfloor$ . For each subsampling method, we select a subset from the training set leading to an estimator  $\widehat{\boldsymbol{\beta}}_{\text{train}}^{(i)}$ , and then use it to predict the response  $\mathbf{y}_{\text{test}}$  in the test set. In this way, PMSE is calculated as

$$\text{PMSE} = \frac{1}{100} \sum_{i=1}^{100} \frac{\|\mathbf{X}_{\text{test}}^{(i)} \widehat{\boldsymbol{\beta}}_{\text{train}}^{(i)} - \mathbf{y}_{\text{test}}^{(i)}\|^2}{\|\mathbf{y}_{\text{test}}^{(i)}\|^2}. \quad (10)$$

PMSE of the full sample OLS estimator (FullOLS) is also provided for comparison. The results of  $\log(\text{MSE})$  and  $\log(\text{PMSE})$  versus different subsample sizes are shown in Figs. 2 and 3, respectively.

In Figs. 2 and 3, we observe that both MSE and PMSE w.r.t. all estimators decreases as  $r$  increases. We also observe that CORE consistently outperforms other subsampling approaches under all circumstances. The advantage becomes more apparent when the level of sparsity increases, i.e., from **R1** to **R5**. Such an observation indicates the proposed estimator can provide a more effective estimate than the competitors, especially when the predictor matrix is of high sparsity. Such success can be attributed to the fact that the proposed core-elements approach can effectively utilize the sparsity structure of the predictor matrix, and the proposed estimator is unbiased and has an approximately minimized estimation variance.

In order to verify the theoretical error bound provided in Theorem 2, we compare the empirical and theoretical values of  $\epsilon$  under different values of  $\epsilon'$ , as shown in Fig. 4. Specifically, given a small  $\epsilon'$ , the empirical value of  $\epsilon$  is calculated as

$$\frac{\|\mathbf{y} - \mathbf{X}\widetilde{\boldsymbol{\beta}}\|^2}{\|\mathbf{y} - \mathbf{X}\widehat{\boldsymbol{\beta}}_{\text{OLS}}\|^2} - 1$$

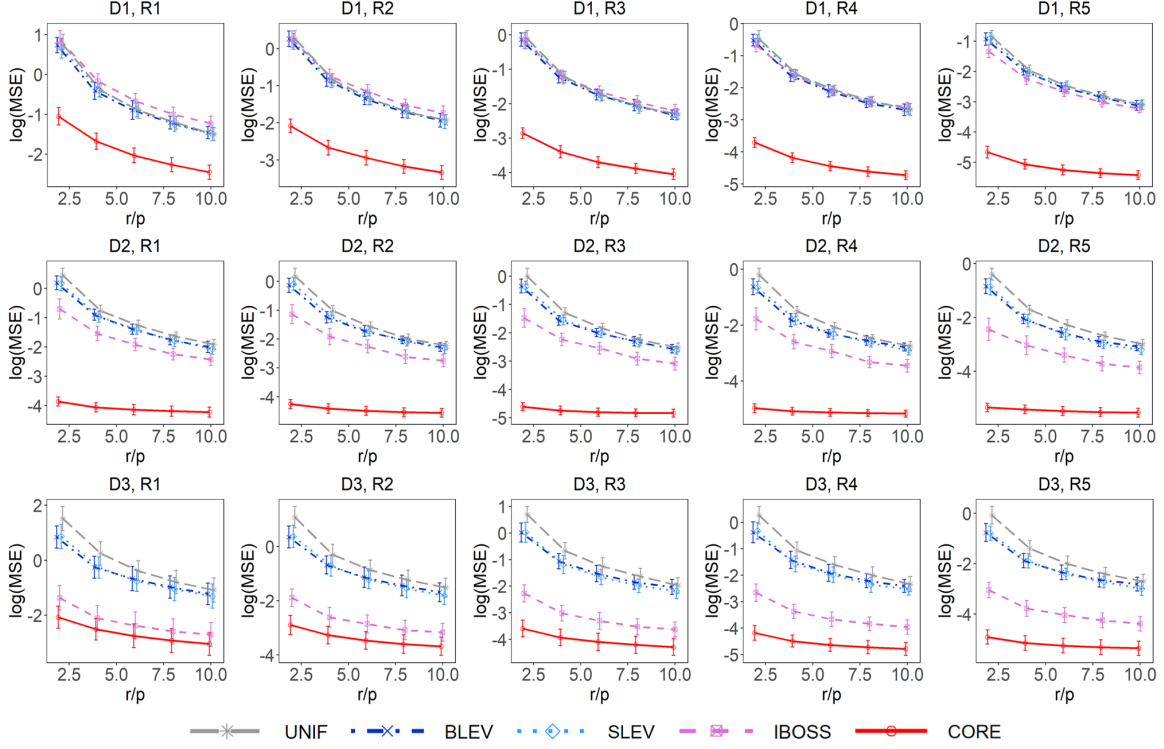


Figure 2: Comparison of different estimators w.r.t. MSE. Each row represents a particular data distribution (**D1-D3**) and each column represents a different sparsity ratio (**R1-R5**). Vertical bars are the standard errors.

according to (7), and the theoretical value of  $\epsilon$  is calculated as

$$\left( \frac{\epsilon' \kappa^2(\mathbf{X})(\kappa^2(\mathbf{X}) + 1) \|\mathbf{y}\|}{(1 - \epsilon' \kappa^2(\mathbf{X})) \|\mathbf{y} - \mathbf{X} \hat{\beta}_{\text{OLS}}\|} \right)^2$$

according to (6). Both  $\epsilon$  and  $\epsilon'$  have been made logarithmic transformation in Fig. 4. We can observe that although the empirical and theoretical values of  $\epsilon$  differs, their growth trends have an apparent parallel pattern. This observation indicates that our proposed error bound and the empirical value are of the same order. Their difference is up to a constant under the log transformation.

## 5.2 Performance on corrupted data

We compare Algorithm 2, referred to as MOM-CORE, with the subsampling methods mentioned above in the presence of outliers. The corrupted data consist of informative

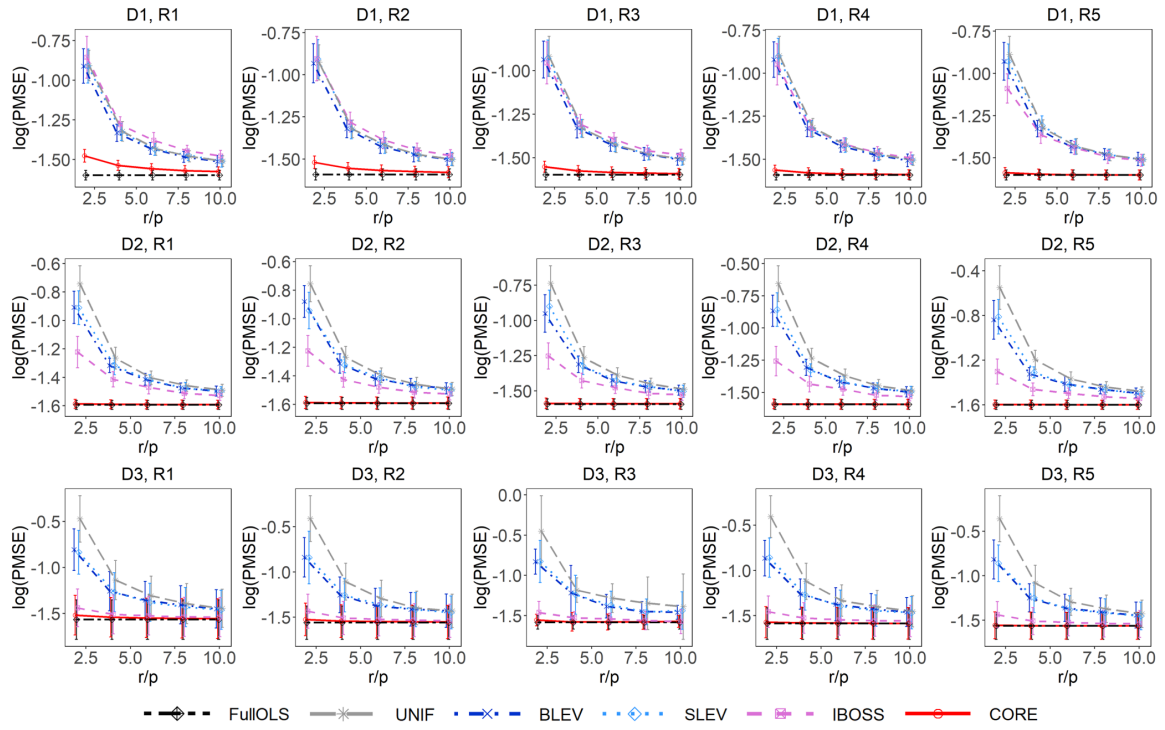


Figure 3: Comparison of different estimators w.r.t. PMSE. Each row represents a particular data distribution (**D1-D3**) and each column represents a different sparsity ratio (**R1-R5**). Vertical bars are the standard errors.

data  $\{(\mathbf{x}_i, y_i)\}_{i \in \mathcal{I}}$  and various types of outliers  $\{(\mathbf{x}_i, y_i)\}_{i \in \mathcal{O}}$  with  $\mathcal{O} = \mathcal{O}_1 \cup \mathcal{O}_2 \cup \mathcal{O}_3 \cup \mathcal{O}_4$ , such that  $|\mathcal{O}| = n_o$  and  $|\mathcal{I}| = n - n_o$ .  $\{(\mathbf{x}_i, y_i)\}_{i \in \mathcal{I}}$  is generated in the same way as in the previous section, and  $\{(\mathbf{x}_i, y_i)\}_{i \in \mathcal{O}}$  is constructed following the setup in [47]. More precisely,

- For  $i \in \mathcal{O}_1$  with  $|\mathcal{O}_1| = \lfloor n_o/4 \rfloor$ ,  $y_i = 1000 + 10\zeta$  and  $\mathbf{x}_i = -10 \times \mathbf{1}_p + \boldsymbol{\zeta}$ , where  $\zeta \in \mathbb{R}$  and  $\boldsymbol{\zeta} \in \mathbb{R}^p$  noises following the (multivariate) standard normal distribution;
- For  $i \in \mathcal{O}_2$  with  $|\mathcal{O}_2| = \lfloor n_o/4 \rfloor$ ,  $y_i = -500 + 10\zeta$  and  $\mathbf{x}_i = 10 \times \mathbf{1}_p + \boldsymbol{\zeta}$ ;
- For  $i \in \mathcal{O}_3$  with  $|\mathcal{O}_3| = \lfloor n_o/4 \rfloor$ ,  $y_i$  is a 0 – 1-Bernoulli random variable and  $\mathbf{x}_i$  is uniformly distributed over  $[0, 1]^p$ ;
- For  $i \in \mathcal{O}_4$ ,  $(\mathbf{x}_i, y_i)$  is generated from the linear model (1) with the same true parameter  $\boldsymbol{\beta} = \mathbf{1}_p$  but for a different choice of design  $\mathbf{X}$  and noise  $\boldsymbol{\varepsilon}$ . Here, we take the covariance matrix  $\boldsymbol{\Sigma}$  as an identity matrix and  $\boldsymbol{\varepsilon}$  is a heavy-tailed noise following  $t_2$

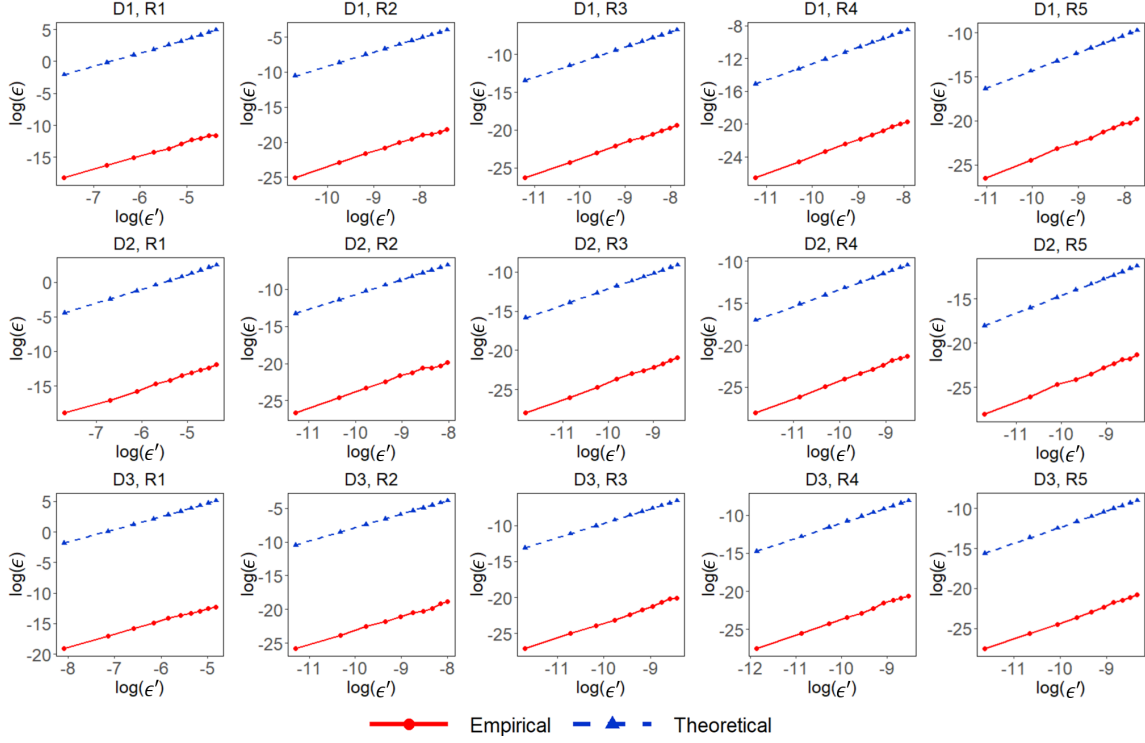


Figure 4: Comparison of the empirical value and the theoretical value of the error term  $\epsilon$ . Each row represents a particular data distribution (**D1-D3**) and each column represents a different sparsity ratio (**R1-R5**).

distribution.

After generating the corrupted data above, observations in  $\mathcal{I}$  and  $\mathcal{O}$  are merged and shuffled before downstream operations. Let the sample size  $n = 10^4$ , the dimension  $p = 20$ , and the number of outliers  $n_o = 20$ . We subsample  $r \in \{5p, 10p, \dots, 25p\}$  rows for row-sampling methods or  $s = rp$  elements for CORE and MOM-CORE. The number of blocks is set to be  $k = 40$  for MOM-CORE. Other settings are the same as those in the above section.

To evaluate the performance of different methods on corrupted data, we calculate MSE according to (9) and PMSE according to (10) for each method, and their results versus increasing subsample sizes are shown in Figs. 5 and 6, respectively. Remark that when predicting the responses, we first split the training set and test set on informative data  $\{(\mathbf{x}_i, y_i)\}_{i \in \mathcal{I}}$ , and then add outliers  $\{(\mathbf{x}_i, y_i)\}_{i \in \mathcal{O}}$  to the training set; that is, the test set is not corrupted by outliers.

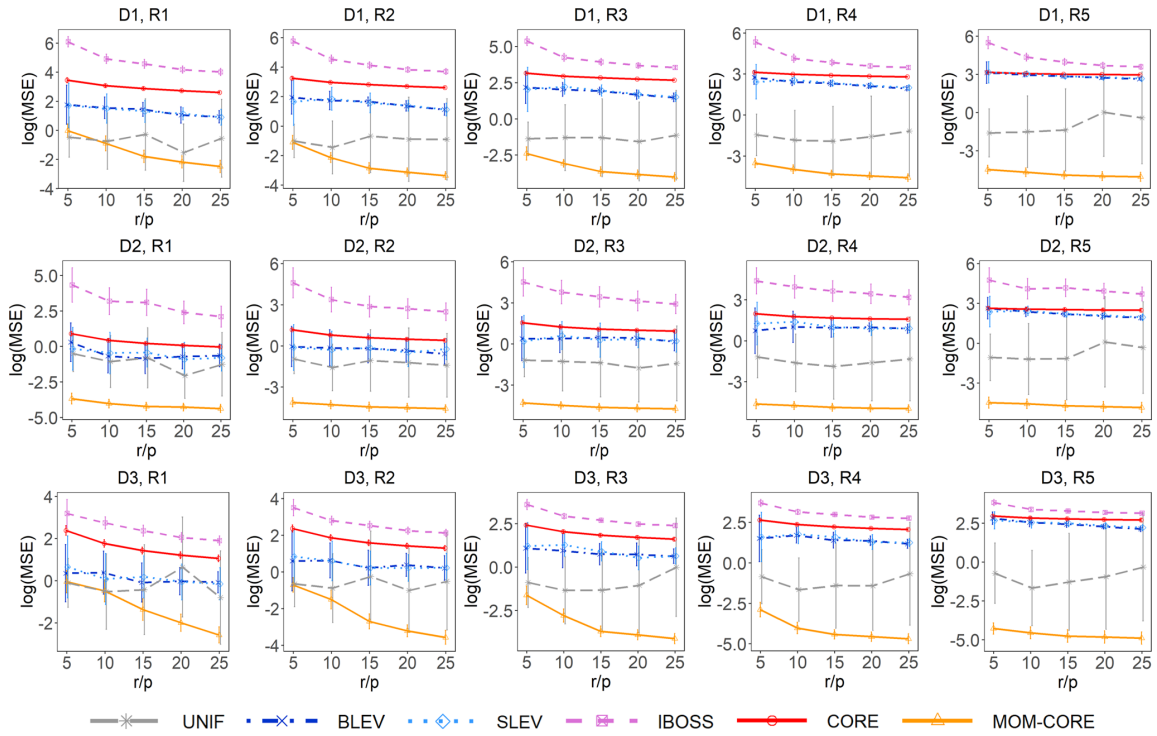


Figure 5: Comparison of different estimators w.r.t. MSE on corrupted data. Each row represents a particular data distribution (**D1-D3**) and each column represents a different sparsity ratio (**R1-R5**). Vertical bars are the standard errors.

As shown in Figs. 5 and 6, MOM-CORE consistently achieves the smallest estimation and prediction error among all these methods, and its advantage becomes more prominent with the increase of sparsity. While other non-uniform subsampling approaches are largely subject to outliers and thus always fail to beat the naive UNIF method. Such an observation indicates that by integrating with the MOM procedure, our proposed MOM core-elements algorithm leads to an effective and robust estimator. It is also worth noting that even the full sample OLS fails to provide successful predictions in the presence of extreme outliers, as shown in Fig. 6. In contrast, the proposed MOM-CORE achieves much more accurate result than FullOLS, requiring less information.

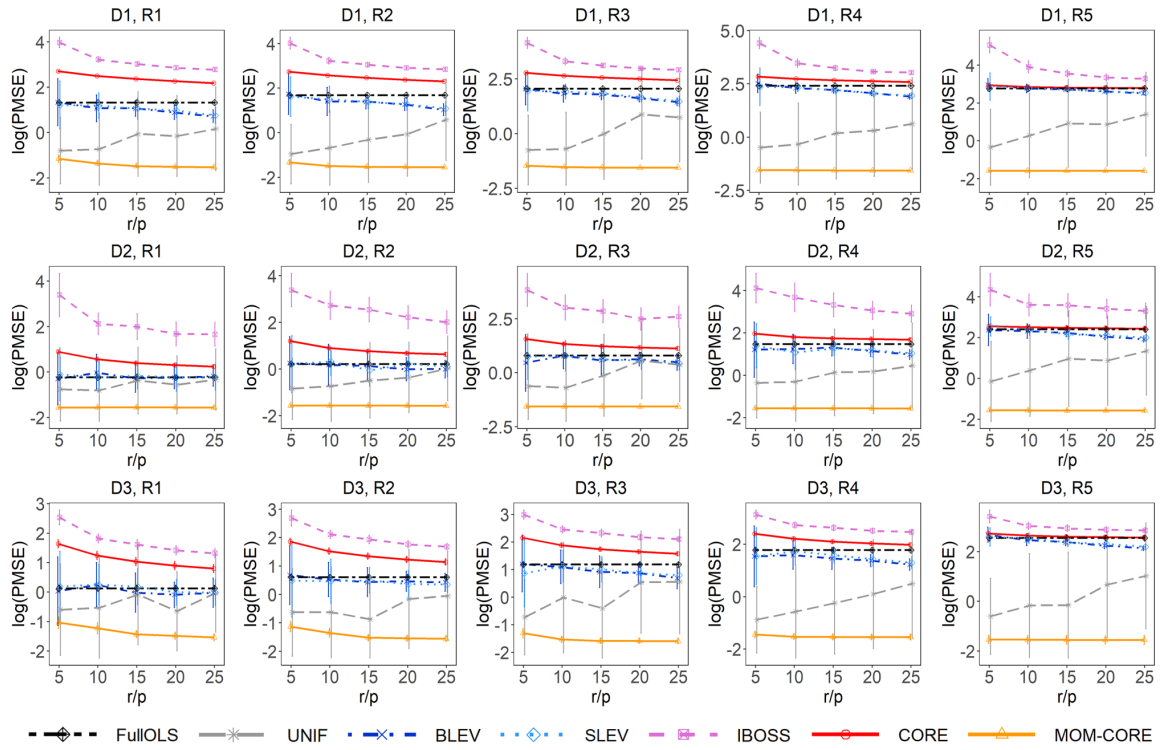


Figure 6: Comparison of different estimators w.r.t. PMSE on corrupted data. Each row represents a particular data distribution (**D1-D3**) and each column represents a different sparsity ratio (**R1-R5**). Vertical bars are the standard errors.

### 5.3 Computing time

To compare the computational efficiency of these subsampling approaches, we present the CPU time (in seconds) for different combinations of the sample size  $n$  and the dimension  $p$  under the case of **D1**, **R1** in Table 1. Here data corruption is not introduced because it hardly affects the computation time. We take the subsample size  $r = 10p$ , and we set the number of blocks  $k = 40$  for MOM-CORE. All computations are implemented using the R programming language [73] on a desktop running Windows 10 with an Intel i5-10210U CPU and 16GB memory. The CPU time for using the full sample is also presented for comparison.

As can be observed from Table 1, all of these estimates are more efficient than the full sample OLS estimate. Among these methods, BLEV and SLEV spend longer CPU time, because they require the calculation of singular value decomposition of the full predictor

Table 1: CPU time (in seconds) of estimating  $\beta$ , for different combinations of  $n$  and  $p$  under **D1**, **R1**.

(a) CPU times for different $p$ , with fixed $n = 10^5$ .							
$p$	UNIF	BLEV	SLEV	IBOSS	CORE	MOM-CORE	FullOLS
50	0.00	0.51	0.51	0.15	0.08	0.13	0.82
100	0.01	2.02	2.03	0.43	0.35	0.38	3.19
500	0.39	46.37	46.39	6.53	5.29	4.72	76.31
(b) CPU times for different $n$ , with fixed $p = 100$ .							
$n$	UNIF	BLEV	SLEV	IBOSS	CORE	MOM-CORE	FullOLS
$5 \times 10^4$	0.00	1.01	1.01	0.12	0.13	0.12	1.72
$5 \times 10^5$	0.02	10.86	10.85	1.36	0.87	0.90	16.95
$5 \times 10^6$	0.11	119.83	119.84	12.94	7.54	9.03	189.65

matrix. We also observe that the proposed CORE and MOM-CORE approaches only require longer times than the UNIF method in almost all circumstances. In addition, their superiority in computation becomes more prominent when  $n$  is much larger than  $p$ , which is exactly the most suitable situation for taking advantage of subsampling.

## 6 Real Data Analysis

In this section, we evaluate the effectiveness of different subsampling methods on two real-world datasets, one highly sparse and the other dense. We assume that the data follow the classical linear model (1). Note that the true coefficients are unknown in real data analysis. Thus we use the full sample ordinary least squares estimator  $\hat{\beta}_{OLS}$  as a surrogate for  $\beta$  when calculating MSE according to (9) based on 100 bootstrap samples. Also, we calculate the PMSE according to (10) to further evaluate the prediction performance. To ensure that OLS is a good oracle, we first remove extreme outliers detected by box-plots, and thus assume that the resultant datasets are not corrupted. The subsampling methods considered here are the same as those in Section 5, and the subsample size is set to be  $r \in \{2p, 4p, \dots, 10p\}$  rows, or  $s = rp$  elements equivalently. We set the number of blocks

for MOM core-elements to be  $k = 5$ .

## 6.1 Example 1: scRNA-seq data

The rapid development of the single-cell RNA sequencing (scRNA-seq) technique enable the gene expression profiling of single cells. ScRNA-seq data are often organized into a reads count matrix, where rows are cells, columns represent genes, and the  $(i, j)$ th component is the observed expression level of the gene  $j$  in cell  $i$ . We consider a scRNA-seq dataset collected by the authors in [10], which includes CD 45+ immune cells from eight breast carcinomas, as well as matched normal breast tissue, blood, and lymph node<sup>1</sup>. Our goal is to find the relationship between the expression of the gene MT-RNR2 and other genes. As a critical neuroprotective factor, the MT-RNR2 gene encodes the Humanin polypeptide and protects against death in Alzheimer’s disease.

To achieve the goal, we take the reads of this gene as the response and the reads for other genes as predictors. Following the data pre-processing steps in [40], we first screen the genes as follows: (1) select top 3,000 genes with the highest expression levels; and (2) select top 500 genes with the largest variances. We then normalize the predictors so that they have unit variance. The distribution of pre-processed data points is shown in Fig. 7(a). The final sample contains  $n \approx 10^5$  cells and  $p = 500$  genes with over 75% zero elements, as illustrated through the histogram in Fig. 7(b).

Figure 7(c) displays the performance of different subsampling approaches for approximating  $\hat{\beta}_{\text{OLS}}$  and predicting  $\mathbf{y}$ , respectively. As there seems to exist no extreme outliers according to Fig. 7(a), CORE and MOM-CORE have nearly identical performances, both of which significantly outperform other subsampling approaches. In addition, the proposed estimators perform almost the same as  $\hat{\beta}_{\text{OLS}}$  w.r.t. the PMSE, even when the selected number of elements is just  $s = 2p^2$ .

---

<sup>1</sup>The dataset is publicly available with the accession code GSE114725 in Gene Expression Omnibus [27].



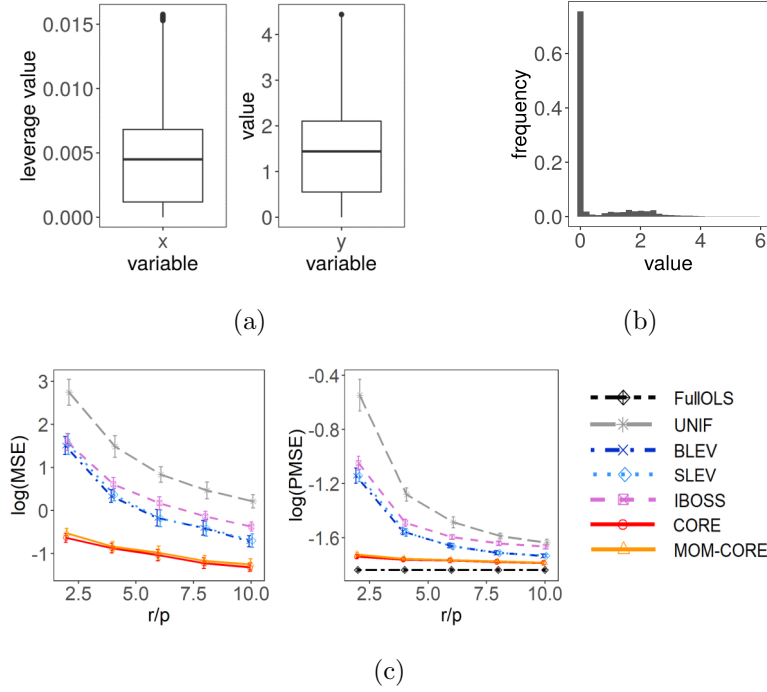


Figure 7: (a) An illustration of predictor leverage values (**left**) and response values (**right**). (b) An illustration of values in the predictor matrix. (c) Comparison of different methods on estimation (**left**) and prediction (**right**) for the scRNA dataset.

Table 2: CPU time (in seconds) of estimating  $\beta$  for the scRNA-seq dataset.

Method	UNIF	BLEV	SLEV	IBOSS	CORE	MOM-CORE	FullOLS
$r = 2p$	0.19	46.98	46.96	8.27	3.24	2.80	-
$r = 6p$	0.61	47.16	47.17	8.89	5.59	4.40	-
$r = 10p$	1.01	47.60	47.62	10.90	7.16	6.42	-
$n$	-	-	-	-	-	-	80.24

Table 2 shows the CPU time for these subsampling methods. Compared to the full sample estimate, all the subsample estimates require a shorter computational time. Similar to the results in Table 1, we observe that the proposed CORE and MOM-CORE methods have great advantages in computing, which is only slower than the naive UNIF method. The results in Fig. 7(c) and Table 2 indicate that the proposed strategy can provide a more effective estimate than the competitors, requiring a relatively short computational time.

## 6.2 Example 2: Higgs bosons data

Physics experiments have been carried out using modern accelerators to produce exotic particles, e.g., Higgs bosons. Observations of these particles and measurements of their properties may yield critical insights into the fundamental properties of the physical universe. Thus, identifying collisions that produce particles of interest has become a fundamental scientific problem, requiring developing high-level features from some kinematic properties measured by the particle detectors in the accelerator.

Our goal is to prevent the need for physicists to derive such high-level features manually. We consider a dataset generated by Monte Carlo simulations [11], and we aim to use all the 21 low-level features as covariates to predict a high-level feature  $m_{jlv}$ , whose distributions are displayed in Fig. 8(a). We refer to the original paper for more detailed information on these features. The predictor matrix is of the size  $n = 1.1 \times 10^7$  and  $p = 21$ , and its values are illustrated through the histogram in Fig. 8(b). One can observe that this predictor matrix is dense.

We then use the subsampling methods to approximate the OLS estimate, and the results of MSE and PMSE are presented in Fig. 8(c). Similar to the results in Fig. 7(c), CORE-based approaches consistently outperform the others though the predictor matrix is completely dense. Considering the CPU time in Table 3, all the subsampling methods compute faster than the full sample OLS estimator, and the proposed CORE approach takes only half the CPU time of the IBOSS method. One can see that core-elements not only achieve satisfactory estimation accuracy but also require a short CPU time, even for a dense dataset.

## 7 Concluding Remarks

Releasing the gaps of element-wise subset selection methods in large-scale data analysis, we developed the core-elements method for least squares estimation. Theoretically, we showed

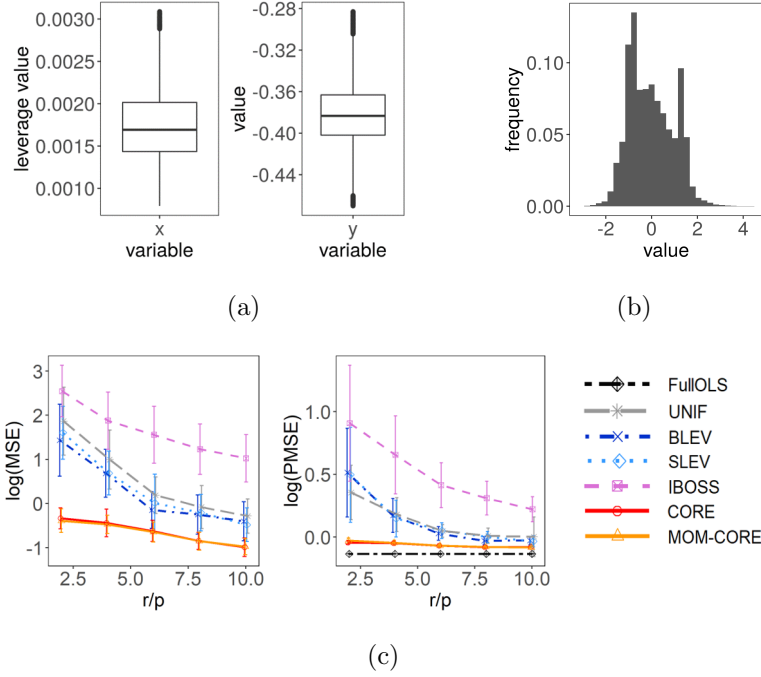


Figure 8: (a) An illustration of predictor leverage values (**left**) and response values (**right**). (b) An illustration of values in the predictor matrix. (c) Comparison of different methods on estimation (**left**) and prediction (**right**) for the Higgs dataset.

Table 3: CPU time (in seconds) of estimating  $\beta$  for the Higgs dataset.

Method	UNIF	BLEV	SLEV	IBOSS	CORE	MOM-CORE	FullOLS
$r = 2p$	0.001	16.77	16.77	7.34	3.00	4.19	-
$r = 6p$	0.001	16.78	16.77	7.45	3.05	4.53	-
$r = 10p$	0.003	16.78	16.78	7.54	3.14	4.90	-
$n$	-	-	-	-	-	-	21.96

that the proposed core-elements estimator approximately minimizes an upper bound of the estimation variance. We also provided a coresets-like finite-sample bound for the proposed estimator, and such a bound is supported by empirical results. To deal with data corruption, we introduced the median-of-means estimation to provide a robust version of core-elements and established consistency of the resultant estimator. Both simulation study and real data analysis suggest that the proposed method is not only suitable for (numerically) sparse matrices, but also has a superior performance for more general dense cases in terms of both estimation error and computing time.

In the future, we will extend core-elements to more general applications, such as generalized linear models, nonparametric models, kernel methods, etc. More importantly, the core-elements approach not only speeds up computation, but also has great applications in preserving data privacy and improving communication efficiency in federated learning, which is also left to our future work.

## SUPPLEMENTARY MATERIAL

In the Supplementary Material, we provide proofs to the theoretical results stated within the manuscript.

## 8 Proofs

### 8.1 Proof of Lemma 1

*Proof.* The variance of  $\tilde{\beta}$  can be organized as

$$\begin{aligned}
\mathbb{E}(\|\tilde{\beta} - \beta\|^2) &= \mathbb{E}\{((\mathbf{X}^{*\top}\mathbf{X})^{-1}\mathbf{X}^{*\top}\mathbf{y} - \beta)^\top((\mathbf{X}^{*\top}\mathbf{X})^{-1}\mathbf{X}^{*\top}\mathbf{y} - \beta)\} \\
&= \mathbb{E}(\mathbf{y}^\top \mathbf{X}^* (\mathbf{X}^\top \mathbf{X}^*)^{-1} (\mathbf{X}^{*\top} \mathbf{X})^{-1} \mathbf{X}^{*\top} \mathbf{y}) - \beta^\top \beta \\
&= \sigma^2 \|(\mathbf{X}^{*\top} \mathbf{X})^{-1} \mathbf{X}^{*\top}\|_F^2.
\end{aligned} \tag{11}$$

The last equality is due to

$$\mathbb{E}(\mathbf{y}^\top \mathbf{A} \mathbf{y}) = (\mathbf{X}\beta)^\top \mathbf{A} \mathbf{X}\beta + \sigma^2 \text{tr}(\mathbf{A})$$

with

$$\mathbf{A} = \mathbf{X}^* (\mathbf{X}^\top \mathbf{X}^*)^{-1} (\mathbf{X}^{*\top} \mathbf{X})^{-1} \mathbf{X}^{*\top}.$$

Considering (11), we have

$$\begin{aligned}
& \|(\mathbf{X}^{*\top} \mathbf{X})^{-1} \mathbf{X}^{*\top}\|_F^2 \\
&= \text{tr}\{(\mathbf{X} - \mathbf{L})(\mathbf{X}^\top \mathbf{X} - \mathbf{X}^\top \mathbf{L})(\mathbf{X}^\top \mathbf{X} - \mathbf{L}^\top \mathbf{X})^{-1}(\mathbf{X} - \mathbf{L})^\top\} \\
&= \text{tr}\{(\mathbf{X} - \mathbf{L})(\mathbf{X}^\top \mathbf{X})^{-1}(\mathbf{I}_p - \mathbf{X}^\top \mathbf{L}(\mathbf{X}^\top \mathbf{X})^{-1})^{-1}(\mathbf{I}_p - (\mathbf{X}^\top \mathbf{X})^{-1} \mathbf{L}^\top \mathbf{X})^{-1}(\mathbf{X}^\top \mathbf{X})^{-1}(\mathbf{X} - \mathbf{L})^\top\} \\
&= \text{tr}\{(\mathbf{I}_p - \mathbf{X}^\top \mathbf{L}(\mathbf{X}^\top \mathbf{X})^{-1})^{-1}(\mathbf{I}_p - (\mathbf{X}^\top \mathbf{X})^{-1} \mathbf{L}^\top \mathbf{X})^{-1}(\mathbf{X}^\top \mathbf{X})^{-1}(\mathbf{X} - \mathbf{L})^\top(\mathbf{X} - \mathbf{L})(\mathbf{X}^\top \mathbf{X})^{-1}\} \\
&= \text{tr}(\mathbf{S}_1 \mathbf{S}_2),
\end{aligned}$$

where

$$\mathbf{S}_1 = (\mathbf{I}_p - \mathbf{X}^\top \mathbf{L}(\mathbf{X}^\top \mathbf{X})^{-1})^{-1} (\mathbf{I}_p - (\mathbf{X}^\top \mathbf{X})^{-1} \mathbf{L}^\top \mathbf{X})^{-1}$$

and

$$\mathbf{S}_2 = (\mathbf{X}^\top \mathbf{X})^{-1}(\mathbf{X} - \mathbf{L})^\top(\mathbf{X} - \mathbf{L})(\mathbf{X}^\top \mathbf{X})^{-1}.$$

First, we consider the term  $\mathbf{S}_1$ . Performing a Taylor expansion of  $(\mathbf{I}_p - (\mathbf{X}^\top \mathbf{X})^{-1} \mathbf{L}^\top \mathbf{X})^{-1}$  around the point  $\mathbf{L} = \mathbf{0}_{p \times p}$  yields

$$(\mathbf{I}_p - (\mathbf{X}^\top \mathbf{X})^{-1} \mathbf{L}^\top \mathbf{X})^{-1} = \mathbf{I}_p + (\mathbf{X}^\top \mathbf{X})^{-1} \mathbf{L}^\top \mathbf{X} + \mathbf{W}_1$$

under the convergence condition that the spectral radius  $\|(\mathbf{X}^\top \mathbf{X})^{-1} \mathbf{L}^\top \mathbf{X}\|_2 = \lambda_0 < 1$  (see Chapter 1, [38]). Then, the remainder satisfies  $\|\mathbf{W}_1\|_2 = O(\lambda_0^2)$  and thus  $\text{tr}(\mathbf{W}_1) \leq pO(\lambda_0^2)$ . Based on the result of Taylor expansion, we have

$$\begin{aligned}
\mathbf{S}_1 &= (\mathbf{I}_p + \mathbf{X}^\top \mathbf{L}(\mathbf{X}^\top \mathbf{X})^{-1} + \mathbf{W}_1^\top) (\mathbf{I}_p + (\mathbf{X}^\top \mathbf{X})^{-1} \mathbf{L}^\top \mathbf{X} + \mathbf{W}_1) \\
&= \mathbf{I}_p + \mathbf{X}^\top \mathbf{L}(\mathbf{X}^\top \mathbf{X})^{-1} + (\mathbf{X}^\top \mathbf{X})^{-1} \mathbf{L}^\top \mathbf{X} + \mathbf{W}_2
\end{aligned}$$

with

$$\mathbf{W}_2 = \mathbf{W}_1 + \mathbf{W}_1^\top + \mathbf{W}_1^\top \mathbf{W}_1 + \mathbf{W}_1^\top (\mathbf{X}^\top \mathbf{X})^{-1} \mathbf{L}^\top \mathbf{X} + \mathbf{X}^\top \mathbf{L}(\mathbf{X}^\top \mathbf{X})^{-1} \mathbf{W}_1 + \mathbf{X}^\top \mathbf{L}(\mathbf{X}^\top \mathbf{X})^{-2} \mathbf{L}^\top \mathbf{X}.$$

One can see that  $\|\mathbf{W}_2\|_2 = O(\lambda_0^2)$ , and thus  $\text{tr}(\mathbf{W}_2) \leq pO(\lambda_0^2)$ . Consequently, we have

$$\text{tr}(\mathbf{S}_1) \leq p + pO(\lambda_0). \quad (12)$$

Next, we consider the other term,  $\mathbf{S}_2$ . It holds that

$$\mathbf{S}_2 = \{\mathbf{I}_p - (\mathbf{X}^\top \mathbf{X})^{-1} \mathbf{L}^\top \mathbf{X} - (\mathbf{X}^\top \mathbf{X})^{-1} \mathbf{X}^\top \mathbf{L} + (\mathbf{X}^\top \mathbf{X})^{-1} \mathbf{L}^\top \mathbf{L}\} (\mathbf{X}^\top \mathbf{X})^{-1}.$$

Note that for real positive semi-definite matrices  $\mathbf{A}$  and  $\mathbf{B}$ , it can be shown that  $\text{tr}(\mathbf{AB}) \leq \text{tr}(\mathbf{A}) \text{tr}(\mathbf{B})$  [84]. Thus,

$$\text{tr}(\mathbf{S}_2) \leq \text{tr}((\mathbf{X}^\top \mathbf{X})^{-1}) \{p + pO(\lambda_0) + \text{tr}((\mathbf{X}^\top \mathbf{X})^{-1} \mathbf{L}^\top \mathbf{L})\}. \quad (13)$$

For positive semi-definite matrices  $\mathbf{S}_1$  and  $\mathbf{S}_2$ , combining (12) and (13) yields

$$\begin{aligned} \text{tr}(\mathbf{S}_1 \mathbf{S}_2) &\leq \text{tr}(\mathbf{S}_1) \text{tr}(\mathbf{S}_2) \\ &\leq \text{tr}((\mathbf{X}^\top \mathbf{X})^{-1}) \{p^2(1 + O(\lambda_0)) + p(1 + O(\lambda_0)) \text{tr}((\mathbf{X}^\top \mathbf{X})^{-1} \mathbf{L}^\top \mathbf{L})\}. \end{aligned}$$

Therefore, we conclude that

$$\begin{aligned} \|(\mathbf{X}^{*\top} \mathbf{X})^{-1} \mathbf{X}^{*\top}\|_F^2 &\leq \text{tr}((\mathbf{X}^\top \mathbf{X})^{-1}) \{p^2(1 + O(\lambda_0)) + p(1 + O(\lambda_0)) \text{tr}((\mathbf{X}^\top \mathbf{X})^{-1} \mathbf{L}^\top \mathbf{L})\} \\ &\leq \text{tr}((\mathbf{X}^\top \mathbf{X})^{-1}) \{p^2(1 + O(\lambda_0)) + p(1 + O(\lambda_0)) \text{tr}((\mathbf{X}^\top \mathbf{X})^{-1}) \|\mathbf{L}\|_F^2\} \\ &= p \left[ \text{tr}((\mathbf{X}^\top \mathbf{X})^{-1}) \{ (p + \text{tr}((\mathbf{X}^\top \mathbf{X})^{-1}) \|\mathbf{L}\|_F^2) (1 + O(\lambda_0)) \} \right]. \end{aligned}$$

□

## 8.2 Proof of Theorem 2

*Proof.* (1) Recalling the definition of OLS estimation, i.e.,

$$\hat{\boldsymbol{\beta}}_{OLS} = \arg \min_{\boldsymbol{\theta} \in \mathbb{R}^p} \|\mathbf{y} - \mathbf{X}\boldsymbol{\theta}\|^2,$$

the left-hand side of inequality is obviously established.

(2) For the right-hand side of inequality,

$$\begin{aligned} &\|\mathbf{y} - \mathbf{X}\tilde{\boldsymbol{\beta}}\|^2 \\ &= \|\mathbf{y} - \mathbf{X}\hat{\boldsymbol{\beta}}_{OLS}\|^2 + 2(\mathbf{y} - \mathbf{X}\hat{\boldsymbol{\beta}}_{OLS})^\top (\mathbf{X}\hat{\boldsymbol{\beta}}_{OLS} - \mathbf{X}\tilde{\boldsymbol{\beta}}) + \|\mathbf{X}\hat{\boldsymbol{\beta}}_{OLS} - \mathbf{X}\tilde{\boldsymbol{\beta}}\|^2 \\ &= \|\mathbf{y} - \mathbf{X}\hat{\boldsymbol{\beta}}_{OLS}\|^2 + \|\mathbf{X}\hat{\boldsymbol{\beta}}_{OLS} - \mathbf{X}\tilde{\boldsymbol{\beta}}\|^2. \end{aligned}$$

The last equality holds because the cross term  $(\mathbf{y} - \mathbf{X}\hat{\boldsymbol{\beta}}_{OLS})^\top (\mathbf{X}\hat{\boldsymbol{\beta}}_{OLS} - \mathbf{X}\tilde{\boldsymbol{\beta}})$  equals to 0.

Thus, it is sufficient to show that

$$\|\mathbf{X}\hat{\boldsymbol{\beta}}_{OLS} - \mathbf{X}\tilde{\boldsymbol{\beta}}\|^2 \leq \epsilon \|\mathbf{y} - \mathbf{X}\hat{\boldsymbol{\beta}}_{OLS}\|^2. \quad (14)$$

Simple algebra yields that

$$\begin{aligned} \|\mathbf{X}\hat{\boldsymbol{\beta}} - \mathbf{X}\tilde{\boldsymbol{\beta}}\|^2 &= \|\mathbf{X}(\mathbf{X}^\top \mathbf{X})^{-1} \mathbf{X}^\top \mathbf{y} - \mathbf{X}(\mathbf{X}^{*\top} \mathbf{X})^{-1} \mathbf{X}^{*\top} \mathbf{y}\|^2 \\ &\leq \|\mathbf{X}(\mathbf{X}^\top \mathbf{X})^{-1} \mathbf{X}^\top - \mathbf{X}(\mathbf{X}^{*\top} \mathbf{X})^{-1} \mathbf{X}^{*\top}\|_2^2 \|\mathbf{y}\|^2. \end{aligned} \quad (15)$$

Then, we consider the term  $\|\mathbf{X}(\mathbf{X}^\top \mathbf{X})^{-1} \mathbf{X}^\top - \mathbf{X}(\mathbf{X}^{*\top} \mathbf{X})^{-1} \mathbf{X}^{*\top}\|_2^2$ . Recall that  $\mathbf{L} = \mathbf{X} - \mathbf{X}^*$ .

By using the condition  $\|\mathbf{L}\|_2 < \epsilon' \|\mathbf{X}\|_2$ , we have

$$\begin{aligned} &\|\mathbf{X}(\mathbf{X}^\top \mathbf{X})^{-1} \mathbf{X}^\top - \mathbf{X}(\mathbf{X}^{*\top} \mathbf{X})^{-1} \mathbf{X}^{*\top}\|_2 \\ &= \|\mathbf{X}(\mathbf{X}^\top \mathbf{X})^{-1} \mathbf{X}^\top - \mathbf{X}[(\mathbf{X} - \mathbf{L})^\top \mathbf{X}]^{-1} (\mathbf{X} - \mathbf{L})^\top\|_2 \\ &= \|\mathbf{X}[(\mathbf{X}^\top \mathbf{X})^{-1} - (\mathbf{X}^\top \mathbf{X} - \mathbf{L}^\top \mathbf{X})^{-1}] \mathbf{X}^\top + \mathbf{X}(\mathbf{X}^\top \mathbf{X} - \mathbf{L}^\top \mathbf{X})^{-1} \mathbf{L}^\top\|_2 \\ &\leq \|\mathbf{X}\|_2^2 \|(\mathbf{X}^\top \mathbf{X})^{-1} - (\mathbf{X}^\top \mathbf{X} - \mathbf{L}^\top \mathbf{X})^{-1}\|_2 + \epsilon' \|\mathbf{X}\|_2^2 \|(\mathbf{X}^\top \mathbf{X} - \mathbf{L}^\top \mathbf{X})^{-1}\|_2 \\ &\leq \lambda_0 \|\mathbf{X}\|_2^2 \|(\mathbf{X}^\top \mathbf{X} - \mathbf{L}^\top \mathbf{X})^{-1}\|_2 + \epsilon' \|\mathbf{X}\|_2^2 \|(\mathbf{X}^\top \mathbf{X} - \mathbf{L}^\top \mathbf{X})^{-1}\|_2 \\ &= (\lambda_0 + \epsilon') \|\mathbf{X}\|_2^2 \|(\mathbf{X}^\top \mathbf{X} - \mathbf{L}^\top \mathbf{X})^{-1}\|_2, \end{aligned} \quad (16)$$

where  $\lambda_0 = \|(\mathbf{X}^\top \mathbf{X})^{-1} \mathbf{L}^\top \mathbf{X}\|_2$ . The last inequality is due to  $\mathbf{A}^{-1} - \mathbf{B}^{-1} = \mathbf{A}^{-1}(\mathbf{B} - \mathbf{A})\mathbf{B}^{-1}$  and then  $\|\mathbf{A}^{-1} - \mathbf{B}^{-1}\|_2 \leq \|\mathbf{A}^{-1}(\mathbf{B} - \mathbf{A})\|_2 \|\mathbf{B}^{-1}\|_2$ .

Consider the term  $\|(\mathbf{X}^\top \mathbf{X} - \mathbf{L}^\top \mathbf{X})^{-1}\|_2$  in (16). A special case of Woodbury formula [35] takes the form  $(\mathbf{A} - \mathbf{B})^{-1} = \mathbf{A}^{-1} + \mathbf{A}^{-1} \mathbf{B} (\mathbf{A} - \mathbf{B})^{-1}$ , which has a recursive structure that yields

$$(\mathbf{A} - \mathbf{B})^{-1} = \sum_{k=0}^{\infty} (\mathbf{A}^{-1} \mathbf{B})^k \mathbf{A}^{-1}. \quad (17)$$

By using (17), it follows that

$$(\mathbf{X}^\top \mathbf{X} - \mathbf{L}^\top \mathbf{X})^{-1} = \sum_{k=0}^{\infty} ((\mathbf{X}^\top \mathbf{X})^{-1} \mathbf{L}^\top \mathbf{X})^k (\mathbf{X}^\top \mathbf{X})^{-1}.$$

Thus, we have

$$\begin{aligned}\|(\mathbf{X}^\top \mathbf{X} - \mathbf{L}^\top \mathbf{X})^{-1}\|_2 &\leq \sum_{k=0}^{\infty} \|(\mathbf{X}^\top \mathbf{X})^{-1} \mathbf{L}^\top \mathbf{X}\|_2^k \|(\mathbf{X}^\top \mathbf{X})^{-1}\|_2 \\ &= \frac{1}{1 - \lambda_0} \|(\mathbf{X}^\top \mathbf{X})^{-1}\|_2.\end{aligned}$$

In this way, the formula (16) can be further bounded by

$$\|\mathbf{X}(\mathbf{X}^\top \mathbf{X})^{-1} \mathbf{X}^\top - \mathbf{X}(\mathbf{X}^{*\top} \mathbf{X})^{-1} \mathbf{X}^{*\top}\|_2 \leq \frac{\lambda_0 + \epsilon'}{1 - \lambda_0} \|\mathbf{X}\|_2^2 \|(\mathbf{X}^\top \mathbf{X})^{-1}\|_2 = \frac{\lambda_0 + \epsilon'}{1 - \lambda_0} \kappa^2(\mathbf{X}), \quad (18)$$

where  $\kappa(\mathbf{X}) = \sigma_{\max}(\mathbf{X})/\sigma_{\min}(\mathbf{X})$  is the condition number of  $\mathbf{X}$ .

Considering  $\lambda_0$ , we have

$$\lambda_0 = \|(\mathbf{X}^\top \mathbf{X})^{-1} \mathbf{L}^\top \mathbf{X}\|_2 \leq \epsilon' \|(\mathbf{X}^\top \mathbf{X})^{-1}\|_2 \|\mathbf{X}\|_2^2 = \epsilon' \kappa^2(\mathbf{X}). \quad (19)$$

Combining (15), (18) and (19), we conclude that if  $\epsilon'$  satisfies

$$\frac{(\kappa^2(\mathbf{X}) + 1)\epsilon'}{1 - \epsilon' \kappa^2(\mathbf{X})} \kappa^2(\mathbf{X}) \leq \frac{\epsilon^{1/2} \|\mathbf{y} - \mathbf{X} \hat{\boldsymbol{\beta}}_{OLS}\|}{\|\mathbf{y}\|} \quad (20)$$

and

$$\epsilon' < \frac{1}{\kappa^2(\mathbf{X})}, \quad (21)$$

then the desired inequality (14) holds. The inequality (21) is required to ensure the upper bound (19) of  $\lambda_0$  is smaller than 1. Further, the inequality (20) can be rewritten as

$$\epsilon' \leq \frac{1}{\kappa^2(\mathbf{X})} \left( 1 + \frac{(\kappa^2(\mathbf{X}) + 1) \|\mathbf{y}\|}{\epsilon^{1/2} \|\mathbf{y} - \mathbf{X} \hat{\boldsymbol{\beta}}_{OLS}\|} \right)^{-1} < \frac{1}{\kappa^2(\mathbf{X})}.$$

This complete the proof of the right-hand side of inequality.  $\square$

### 8.3 Proof of Theorem 3

*Proof.* Since the dimension of the parameter  $\boldsymbol{\beta}$  is finite and the MOM procedure is adopted coordinate-wisely, without loss of generality, we only prove the univariate case, and we assume the first block contains no outliers.



By the definition of MOM, one can see that

$$\left\{ \|\tilde{\boldsymbol{\beta}}_{\text{MOM}} - \boldsymbol{\beta}\| > \epsilon \right\} \subseteq \left\{ \sum_{l=1}^k I(\|\tilde{\boldsymbol{\beta}}^{(l)} - \boldsymbol{\beta}\| > \epsilon) \geq k/2 \right\},$$

where  $I(\cdot)$  is the indicator function and  $\tilde{\boldsymbol{\beta}}^{(l)}$  is the core-elements estimator on the  $l$ th block.

To ease the conversation, denote  $Z^{(l)} = I(\|\tilde{\boldsymbol{\beta}}^{(l)} - \boldsymbol{\beta}\| > \epsilon)$  and  $\mathcal{B}_{\mathcal{O}}^c$  be the complementary set of  $\mathcal{B}_{\mathcal{O}}$ , i.e.,  $\mathcal{B}_{\mathcal{O}}^c = \{1, \dots, k\} \setminus \mathcal{B}_{\mathcal{O}}$ . Then, we have

$$\begin{aligned} \mathbb{P}(\|\tilde{\boldsymbol{\beta}}_{\text{MOM}} - \boldsymbol{\beta}\| > \epsilon) &\leq \mathbb{P}\left(\sum_{l=1}^k I(\|\tilde{\boldsymbol{\beta}}^{(l)} - \boldsymbol{\beta}\| > \epsilon) \geq k/2\right) \\ &= \mathbb{P}\left(\sum_{l \in \mathcal{B}_{\mathcal{O}}^c} Z^{(l)} + \sum_{l \in \mathcal{B}_{\mathcal{O}}} Z^{(l)} \geq k/2\right) \\ &\leq \mathbb{P}\left(\sum_{l \in \mathcal{B}_{\mathcal{O}}^c} Z^{(l)} + |\mathcal{B}_{\mathcal{O}}| \geq k/2\right) \\ &= \mathbb{P}\left(\frac{1}{k - |\mathcal{B}_{\mathcal{O}}|} \sum_{l \in \mathcal{B}_{\mathcal{O}}^c} (Z^{(l)} - \mathbb{E}(Z^{(l)})) \geq \frac{k - 2|\mathcal{B}_{\mathcal{O}}|}{2(k - |\mathcal{B}_{\mathcal{O}}|)} - \mathbb{E}(Z^{(1)})\right) \quad (22) \end{aligned}$$

$$\leq \exp\left\{-2(k - |\mathcal{B}_{\mathcal{O}}|) \left(\frac{1}{2} - \frac{|\mathcal{B}_{\mathcal{O}}|}{2(k - |\mathcal{B}_{\mathcal{O}}|)} - \mathbb{E}(Z^{(1)})\right)^2\right\}, \quad (23)$$

where (22) comes from the fact that the partition is random, so that  $\tilde{\boldsymbol{\beta}}^{(l)}$  are i.i.d. for  $l \in \mathcal{B}_{\mathcal{O}}^c$ , which indicates  $\mathbb{E}(Z^{(l)}) = \mathbb{E}(Z^{(1)})$  for all  $l \in \mathcal{B}_{\mathcal{O}}^c$ ; the inequality (23) comes from the Hoeffding's inequality.

From the Markov's inequality, one can see that

$$\mathbb{E}(Z^{(1)}) \leq \mathbb{E}(\|\tilde{\boldsymbol{\beta}}^{(1)} - \boldsymbol{\beta}\|^2)/\epsilon^2 \rightarrow 0$$

according to Lemma 1 under (H.1)–(H.3). Note that  $|\mathcal{B}_{\mathcal{O}}|/(2k - 2|\mathcal{B}_{\mathcal{O}}|) \rightarrow 0$  since  $|\mathcal{B}_{\mathcal{O}}|$  is finite and  $k \rightarrow \infty$ . Thus the desired result follows.  $\square$

## References

- [1] D. Achlioptas, Z. S. Karnin, and E. Liberty. Near-optimal entrywise sampling for data matrices. *Advances in Neural Information Processing Systems*, 26:1565–1573, 2013.

- [2] D. Achlioptas and F. Mcsherry. Fast computation of low-rank matrix approximations. *Journal of the Association for Computing Machinery*, 54(2):1–19, 2007.
- [3] M. Ai, F. Wang, J. Yu, and H. Zhang. Optimal subsampling for large-scale quantile regression. *Journal of Complexity*, 62:101512, 2020.
- [4] M. Ai, J. Yu, H. Zhang, and H. Wang. Optimal subsampling algorithms for big data regressions. *Statistica Sinica*, 31:749–772, 2021.
- [5] A. Alaoui and M. W. Mahoney. Fast randomized kernel ridge regression with statistical guarantees. *Advances in Neural Information Processing Systems*, 28:775–783, 2015.
- [6] N. Alon, Y. Matias, and M. Szegedy. The space complexity of approximating the frequency moments. *Journal of Computer and system sciences*, 58(1):137–147, 1999.
- [7] J. Altschuler, F. Bach, A. Rudi, and J. Niles-Weed. Massively scalable Sinkhorn distances via the Nyström method. *Advances in Neural Information Processing Systems*, 32:4427–4437, 2019.
- [8] S. Arora, E. Hazan, and S. Kale. Fast algorithms for approximate semidefinite programming using the multiplicative weights update method. In *46th Annual IEEE Symposium on Foundations of Computer Science (FOCS’05)*, pages 339–348. IEEE, 2005.
- [9] S. Arora, E. Hazan, and S. Kale. A fast random sampling algorithm for sparsifying matrices. In *Approximation, Randomization, and Combinatorial Optimization. Algorithms and Techniques*, pages 272–279. Springer, 2006.
- [10] E. Azizi, A. J. Carr, G. Plitas, A. E. Cornish, C. Konopacki, S. Prabhakaran, J. Nainys, K. Wu, V. Kiseliovas, and M. Setty. Single-cell map of diverse immune phenotypes in the breast tumor microenvironment. *Cell*, 174(5):1293–1308, 2018.
- [11] P. Baldi, P. Sadowski, and D. Whiteson. Searching for exotic particles in high-energy physics with deep learning. *Nature Communications*, 5(1):1–9, 2014.
- [12] C. Boutsidis, P. Drineas, and M. Magdon-Ismail. Near-optimal coresets for least-squares regression. *IEEE Transactions on Information Theory*, 59(10):6880–6892, 2013.
- [13] J.-F. Cai, E. J. Candès, and Z. Shen. A singular value thresholding algorithm for matrix completion. *SIAM Journal on Optimization*, 20(4):1956–1982, 2010.

- [14] E. J. Candès and B. Recht. Exact matrix completion via convex optimization. *Foundations of Computational Mathematics*, 9(6):717–772, 2009.
- [15] E. J. Candès and T. Tao. The power of convex relaxation: Near-optimal matrix completion. *IEEE Transactions on Information Theory*, 56(5):2053–2080, 2010.
- [16] Y. Carmon, Y. Jin, A. Sidford, and K. Tian. Coordinate methods for matrix games. In *2020 IEEE 61st Annual Symposium on Foundations of Computer Science (FOCS)*, pages 283–293. IEEE, 2020.
- [17] Y. Chen, S. Bhojanapalli, S. Sanghavi, and R. Ward. Coherent matrix completion. In *International Conference on Machine Learning*, pages 674–682. PMLR, 2014.
- [18] K. L. Clarkson, M. K. Warmuth, M. Mahoney, and M. Dereziński. Minimax experimental design: Bridging the gap between statistical and worst-case approaches to least-squares regression. *Proceedings of Machine Learning Research*, 99:1–20, 2019.
- [19] A. Dasgupta, P. Drineas, B. Harb, R. Kumar, and M. W. Mahoney. Sampling algorithms and coresets for  $l_p$  regression. *SIAM Journal on Computing*, 38(5):2060–2078, 2009.
- [20] T. A. Davis and Y. Hu. The University of Florida sparse matrix collection. *ACM Transactions on Mathematical Software (TOMS)*, 38(1):1–25, 2011.
- [21] M. Dereziński, M. K. Warmuth, and D. J. Hsu. Leveraged volume sampling for linear regression. *Advances in Neural Information Processing Systems*, 31:2510–2519, 2018.
- [22] D. L. Donoho and M. Gasko. Breakdown properties of location estimates based on halfspace depth and projected outlyingness. *The Annals of Statistics*, 20(4):1803–1827, 1992.
- [23] D. L. Donoho and P. J. Huber. The notion of breakdown point. *A Festschrift for Erich L. Lehmann*, 1983.
- [24] P. Drineas, R. Kannan, and M. W. Mahoney. Fast Monte Carlo algorithms for matrices I: Approximating matrix multiplication. *SIAM Journal on Computing*, 36(1):132–157, 2006.
- [25] P. Drineas and A. Zouzias. A note on element-wise matrix sparsification via a matrix-valued Bernstein inequality. *Information Processing Letters*, 111(8):385–389, 2011.
- [26] A. d’Aspremont. Subsampling algorithms for semidefinite programming. *Stochastic Systems*, 1(2):274–305, 2011.

- [27] R. Edgar, M. Domrachev, and A. E. Lash. Gene Expression Omnibus: NCBI gene expression and hybridization array data repository. *Nucleic Acids Research*, 30(1):207–210, 2002.
- [28] N. El Karoui and A. d’Aspremont. Second order accurate distributed eigenvector computation for extremely large matrices. *Electronic Journal of Statistics*, 4:1345–1385, 2010.
- [29] G. Eraslan, L. M. Simon, M. Mircea, N. S. Mueller, and F. J. Theis. Single-cell RNA-seq denoising using a deep count autoencoder. *Nature Communications*, 10(1):1–14, 2019.
- [30] D. Feldman, M. Faulkner, and A. Krause. Scalable training of mixture models via coresets. *Advances in Neural Information Processing Systems*, 24:2142–2150, 2011.
- [31] D. Feldman, M. Schmidt, and C. Sohler. Turning big data into tiny data: Constant-size coresets for  $k$ -means, PCA, and projective clustering. *SIAM Journal on Computing*, 49(3):601–657, 2020.
- [32] D. Garber and E. Hazan. Sublinear time algorithms for approximate semidefinite programming. *Mathematical Programming*, 158(1):329–361, 2016.
- [33] C. Gu and Y.-J. Kim. Penalized likelihood regression: general formulation and efficient approximation. *Canadian Journal of Statistics*, 30(4):619–628, 2002.
- [34] N. Gupta and A. Sidford. Exploiting numerical sparsity for efficient learning: faster eigenvector computation and regression. *Advances in Neural Information Processing Systems*, 31:5274–5283, 2018.
- [35] W. W. Hager. Updating the inverse of a matrix. *SIAM Review*, 31(2):221–239, 1989.
- [36] F. R. Hampel. *Contributions to the Theory of Robust Estimation*. University of California, Berkeley, 1968.
- [37] T. Hastie, R. Mazumder, J. D. Lee, and R. Zadeh. Matrix completion and low-rank SVD via fast alternating least squares. *The Journal of Machine Learning Research*, 16(1):3367–3402, 2015.
- [38] N. J. Higham. *Functions of Matrices: Theory and Computation*. SIAM, 2008.
- [39] D. Hsu and S. Sabato. Heavy-tailed regression with a generalized median-of-means. In *International Conference on Machine Learning*, pages 37–45. PMLR, 2014.

- [40] J. Huang, S. Ma, and C.-H. Zhang. Adaptive Lasso for sparse high-dimensional regression models. *Statistica Sinica*, pages 1603–1618, 2008.
- [41] M. R. Jerrum, L. G. Valiant, and V. V. Vazirani. Random generation of combinatorial structures from a uniform distribution. *Theoretical Computer Science*, 43:169–188, 1986.
- [42] K. S. Jones. A statistical interpretation of term specificity and its application in retrieval. *Journal of Documentation*, 60(5):493–502, 2004.
- [43] P. Kairouz, H. B. McMahan, B. Avent, A. Bellet, M. Bennis, A. N. Bhagoji, K. Bonawitz, Z. Charles, G. Cormode, R. Cummings, et al. Advances and open problems in federated learning. *Foundations and Trends® in Machine Learning*, 14(1–2):1–210, 2021.
- [44] J. Konečný, H. B. McMahan, F. X. Yu, P. Richtárik, A. T. Suresh, and D. Bacon. Federated learning: Strategies for improving communication efficiency. In *NIPS Workshop on Private Multi-Party Machine Learning*, 2016.
- [45] A. Kundu, P. Drineas, and M. Magdon-Ismail. Recovering PCA and sparse PCA via hybrid- $(\ell_1, \ell_2)$  sparse sampling of data elements. *The Journal of Machine Learning Research*, 18(1):2558–2591, 2017.
- [46] G. Lecué and M. Lerasle. Learning from MOM’s principles: Le Cam’s approach. *Stochastic Processes and Their Applications*, 129(11):4385–4410, 2019.
- [47] G. Lecué and M. Lerasle. Robust machine learning by median-of-means: theory and practice. *The Annals of Statistics*, 48(2):906–931, 2020.
- [48] M. Lerasle, Z. Szabó, T. Mathieu, and G. Lecué. MONK outlier-robust mean embedding estimation by median-of-means. In *International Conference on Machine Learning*, pages 3782–3793. PMLR, 2019.
- [49] F. Li, R. Xie, Z. Wang, L. Guo, J. Ye, P. Ma, and W. Song. Online distributed IoT security monitoring with multidimensional streaming big data. *IEEE Internet of Things Journal*, 7(5):4387–4394, 2019.
- [50] N. Li, T. Li, and S. Venkatasubramanian.  $t$ -closeness: Privacy beyond  $k$ -anonymity and  $l$ -diversity. In *2007 IEEE 23rd International Conference on Data Engineering*, pages 106–115. IEEE, 2007.
- [51] T. Li and C. Meng. Modern subsampling methods for large-scale least squares regression. *International Journal of Cyber-Physical Systems (IJCPS)*, 2(2):1–28, 2021.

- [52] M. D. Luecken and F. J. Theis. Current best practices in single-cell RNA-seq analysis: a tutorial. *Molecular Systems Biology*, 15(6):e8746, 2019.
- [53] G. Lugosi and S. Mendelson. Regularization, sparse recovery, and median-of-means tournaments. *Bernoulli*, 25(3):2075–2106, 2019.
- [54] A. T. Lun, K. Bach, and J. C. Marioni. Pooling across cells to normalize single-cell RNA sequencing data with many zero counts. *Genome Biology*, 17(1):1–14, 2016.
- [55] P. Ma, J. Z. Huang, and N. Zhang. Efficient computation of smoothing splines via adaptive basis sampling. *Biometrika*, 102(3):631–645, 2015.
- [56] P. Ma, M. W. Mahoney, and B. Yu. A statistical perspective on algorithmic leveraging. *The Journal of Machine Learning Research*, 16(1):861–911, 2015.
- [57] P. Ma and X. Sun. Leveraging for big data regression. *Wiley Interdisciplinary Reviews: Computational Statistics*, 7(1):70–76, 2015.
- [58] P. Ma, X. Zhang, X. Xing, J. Ma, and M. Mahoney. Asymptotic analysis of sampling estimators for randomized numerical linear algebra algorithms. In *International Conference on Artificial Intelligence and Statistics*, pages 1026–1035. PMLR, 2020.
- [59] T. Mathieu. *M-estimation and Median of Means applied to statistical learning*. PhD thesis, Université Paris-Saclay, 2021.
- [60] C. Meng, Y. Wang, X. Zhang, A. Mandal, W. Zhong, and P. Ma. Effective statistical methods for big data analytics. In *Handbook of Research on Applied Cybernetics and Systems Science*, pages 280–299. IGI Global, 2017.
- [61] C. Meng, R. Xie, A. Mandal, X. Zhang, W. Zhong, and P. Ma. Lowcon: A design-based subsampling approach in a misspecified linear model. *Journal of Computational and Graphical Statistics*, 30(3):694–708, 2021.
- [62] C. Meng, J. Yu, Y. Chen, W. Zhong, and P. Ma. Smoothing splines approximation using Hilbert curve basis selection. *Journal of Computational and Graphical Statistics*, pages 1–11, 2022.
- [63] C. Meng, X. Zhang, J. Zhang, W. Zhong, and P. Ma. More efficient approximation of smoothing splines via space-filling basis selection. *Biometrika*, 107:723–735, 2020.
- [64] A. Munteanu, C. Schwiegelshohn, C. Sohler, and D. P. Woodruff. On coresets for logistic regression. *Advances in Neural Information Processing Systems*, 31:6562–6571, 2018.

- [65] B. Muzellec, J. Josse, C. Boyer, and M. Cuturi. Missing data imputation using optimal transport. In *International Conference on Machine Learning*, pages 7130–7140. PMLR, 2020.
- [66] A. Narayanan and V. Shmatikov. Robust de-anonymization of large sparse datasets. In *2008 IEEE Symposium on Security and Privacy*, pages 111–125. IEEE, 2008.
- [67] S. Qaiser and R. Ali. Text mining: use of TF-IDF to examine the relevance of words to documents. *International Journal of Computer Applications*, 181(1):25–29, 2018.
- [68] J. Ramos. Using TF-IDF to determine word relevance in document queries. In *Proceedings of the 1st Instructional Conference on Machine Learning*, volume 242, pages 29–48. Citeseer, 2003.
- [69] D. Risso, F. Perraudeau, S. Gribkova, S. Dudoit, and J.-P. Vert. A general and flexible method for signal extraction from single-cell RNA-seq data. *Nature Communications*, 9(1):1–17, 2018.
- [70] B. Settles. Active learning. *Synthesis Lectures on Artificial Intelligence and Machine Learning*, 6(1):1–114, 2012.
- [71] D. J. Stekhoven and P. Bühlmann. MissForest—non-parametric missing value imputation for mixed-type data. *Bioinformatics*, 28(1):112–118, 2012.
- [72] X. Sun, W. Zhong, and P. Ma. An asymptotic and empirical smoothing parameters selection method for smoothing spline anova models in large samples. *Biometrika*, 108(1):149–166, 2021.
- [73] R. C. Team et al. R: A language and environment for statistical computing. 2013.
- [74] J. Tu, W. Liu, X. Mao, and X. Chen. Variance reduced median-of-means estimator for byzantine-robust distributed inference. *Journal of Machine Learning Research*, 22(84):1–67, 2021.
- [75] S. Van Buuren and K. Groothuis-Oudshoorn. MICE: Multivariate imputation by chained equations in R. *Journal of statistical software*, 45:1–67, 2011.
- [76] H. Wang, M. Yang, and J. Stufken. Information-based optimal subdata selection for big data linear regression. *Journal of the American Statistical Association*, 114(525):393–405, 2019.
- [77] H. Wang, R. Zhu, and P. Ma. Optimal subsampling for large sample logistic regression. *Journal of the American Statistical Association*, 113(522):829–844, 2018.

- [78] J. Wang, J. Zou, and H. Y. Wang. Sampling with replacement vs Poisson sampling: a comparative study in optimal subsampling. *IEEE Transactions on Information Theory*, 2022.
- [79] S. Wang, A. Gittens, and M. W. Mahoney. Scalable kernel K-means clustering with Nyström approximation: relative-error bounds. *The Journal of Machine Learning Research*, 20(1):431–479, 2019.
- [80] S. Wang and Z. Zhang. Improving CUR matrix decomposition and the Nyström approximation via adaptive sampling. *The Journal of Machine Learning Research*, 14(1):2729–2769, 2013.
- [81] Y. Wang, A. W. Yu, and A. Singh. On computationally tractable selection of experiments in measurement-constrained regression models. *The Journal of Machine Learning Research*, 18(1):5238–5278, 2017.
- [82] C. K. Williams and M. Seeger. Using the Nyström method to speed up kernel machines. *Advances in Neural Information Processing Systems*, 13:682–688, 2000.
- [83] R. Xie, Z. Wang, S. Bai, P. Ma, and W. Zhong. Online decentralized leverage score sampling for streaming multidimensional time series. In *The 22nd International Conference on Artificial Intelligence and Statistics*, pages 2301–2311, 2019.
- [84] X. M. Yang, X. Q. Yang, and K. L. Teo. A matrix trace inequality. *Journal of Mathematical Analysis and Applications*, 263(1):327–331, 2001.
- [85] J. Yu, H. Wang, M. Ai, and H. Zhang. Optimal distributed subsampling for maximum quasi-likelihood estimators with massive data. *Journal of the American Statistical Association*, 117(537):265–276, 2020.
- [86] X. Zhang, R. Xie, and P. Ma. Statistical leveraging methods in big data. In *Handbook of Big Data Analytics*, pages 51–74. Springer, 2018.